

**STUDY OF FEW LAYER GRAPHENE SYNTHESISED BY INTERLAYER  
CATALYTIC EXFOLIATION METHOD**

**CHEN TONG YANG**

**A project report submitted in partial fulfilment of the  
requirements for the award of Bachelor of Engineering  
(Honours) Mechanical Engineering**

**Lee Kong Chian Faculty of Engineering and Science  
Universiti Tunku Abdul Rahman**

**April 2019**

**DECLARATION**

I hereby declare that this project report is based on my original work except for citations and quotations which have been duly acknowledged. I also declare that it has not been previously and concurrently submitted for any other degree or award at UTAR or other institutions.

Signature : \_\_\_\_\_

Name : Chen Tong Yang

ID No. : 14UEB03118

Date : \_\_\_\_\_

**APPROVAL FOR SUBMISSION**

I certify that this project report entitled “**STUDY OF FEW LAYER GRAPHENE SYNTHESISED BY INTERLAYER CATALYTIC EXFOLIATION METHOD**” was prepared by **CHEN TONG YANG** has met the required standard for submission in partial fulfilment of the requirements for the award of Bachelor of Engineering (Honours) Mechanical Engineering at Universiti Tunku Abdul Rahman.

Approved by,

Signature : \_\_\_\_\_

Supervisor : Dr Ting Chen Hunt

Date : \_\_\_\_\_

Signature : \_\_\_\_\_

Co-Supervisor : Ts Dr Yeo Wei Hong

Date : \_\_\_\_\_

The copyright of this report belongs to the author under the terms of the Copyright Act 1987 as qualified by Intellectual Property Policy of Universiti Tunku Abdul Rahman. Due acknowledgement shall always be made of the use of any material contained in, or derived from, this report.

© 2019, Chen Tong Yang. All right reserved.

## ACKNOWLEDGEMENTS

I would like to take this opportunity to utter my utmost gratitude towards everyone that have been contributory and supportive in the successful completion of this final year project as a fractional fulfilment of the requirement for the Bachelor of Engineering (Hons.) Mechanical Engineering in Universiti Tunku Abdul Rahman.

First of all, I would like to express my deepest appreciation to my research supervisor, Dr Ting Chen Hunt and co-supervisor, Ts Dr Yeo Wei Hong for their invaluable guidance, recommendations, advice, insight and enormous patience towards the successful completion of this research.

Next, I would like to convey my gratefulness and thankfulness to UTAR for providing me with the opportunity to get involved in this research project as a requirement for the degree course of engineering.

Furthermore, I would also like to heartily thank my loving family for their love, care and encouragement. Last but not least, I would like to extend my gratitude to my friends and course-mates for teaching and sharing me the practical skills throughout this research period.

## ABSTRACT

Graphite is formed by weak Van der Waals force that connecting two-dimensional graphene layers together and strong covalent bond that forms between the adjacent planes of the carbon atoms that create small carbon to carbon distance. Graphene sheet is an atomic layer of graphite and it is formed by carbon atoms that are arranged in a simple honeycomb or hexagonal lattice. Graphite intercalated compound (GIC), few-layer graphene (FLG) and graphene are the promising materials to improve the storage capacity of capacitor. Even though graphene has the highest energy storage capacity, however, the synthesis cost of graphene is high. In this project, GIC and FLG will be used as the materials to fabricate supercapacitor. The performance of a normal capacitor will be used to compare with the capacitor that is fabricated by using GIC and FLG. The method that was utilised in this project to synthesis FLG was interlayer catalytic exfoliation. Iron (III) chloride graphite intercalated compound ( $FeCl_3 - GIC$ ) can be obtained by intercalating iron (III) chloride ( $FeCl_3$ ) into the layered structure of graphite. In order to obtain iron (III) chloride few-layer graphene ( $FeCl_3 - FLG$ ),  $FeCl_3 - GIC$  had to be ultrasonicated for 3 hours. Next, the synthesised  $FeCl_3 - GIC$  and  $FeCl_3 - FLG$  will then characterise by SEM, FESEM, EDX, XRD and FTIR to validate the results. SEM results of  $FeCl_3 - GIC$  shows that there were  $FeCl_3$  intercalated into the layered structure of graphite and hence formed  $FeCl_3 - GIC$ . Whereas, the SEM and FESEM of  $FeCl_3 - FLG$  show that it is formed by the combination of two to five layers of graphene sheets. The results of EDX and XRD supported the results of SEM and FESEM by proving that there were traces of  $FeCl_3$  found in both  $FeCl_3 - GIC$  and  $FeCl_3 - FLG$  samples. Moreover, FTIR results of  $FeCl_3 - GIC$  and  $FeCl_3 - FLG$  eliminated the possibility of the formation of graphene oxide (GO). The synthesised  $FeCl_3 - GIC$  and  $FeCl_3 - FLG$  were then used as the materials to fabricate supercapacitor. By comparing the performance of normal capacitor and supercapacitors, the results show that  $FeCl_3 - GIC$  supercapacitor was able to store about 30 times more energy than a normal capacitor, whereas  $FeCl_3 - FLG$  supercapacitor is able to store about 70 times more energy than a normal capacitor.  $FeCl_3 - GIC$  and  $FeCl_3 - FLG$  had showed an excellent results on energy storage system, it is definitely a missing puzzle for taking current technology to the next level.

## TABLE OF CONTENTS

<b>DECLARATION</b>	<b>ii</b>
<b>APPROVAL FOR SUBMISSION</b>	<b>iii</b>
<b>ACKNOWLEDGEMENTS</b>	<b>v</b>
<b>ABSTRACT</b>	<b>vi</b>
<b>TABLE OF CONTENTS</b>	<b>vii</b>
<b>LIST OF TABLES</b>	<b>x</b>
<b>LIST OF FIGURES</b>	<b>xi</b>
<b>LIST OF SYMBOLS / ABBREVIATIONS</b>	<b>xiv</b>

### CHAPTER

<b>1</b>	<b>INTRODUCTION</b>	<b>1</b>
	1.1 Introduction	1
	1.2 Importance of the Study	2
	1.3 Problem Statement	2
	1.4 Aim and Objectives	3
	1.5 Scope of Study	3
	1.6 Structure of Thesis	3
<b>2</b>	<b>LITERATURE REVIEW</b>	<b>5</b>
	2.1 Introduction	5
	2.2 Graphite	5
	2.3 Graphite Intercalated Compound	6
	2.4 Graphene	6
	2.4.1 Graphene Properties	7
	2.4.2 Synthesis of graphene	8
	2.5 Graphene Oxide	9
	2.6 Applications of Graphene	10
	2.6.1 Graphene Bulb	10
	2.6.2 Graphene Superconductor	11

2.6.3	Graphene Chip	11
2.6.4	Drug Carrier	12
2.6.5	Hydrogen Storage Materials	13
2.6.6	Graphene Battery	14
2.6.7	Graphene Supercapacitor	15
2.6.8	Graphene Wearable Functional Devices	15
2.7	Graphite Intercalation Methods	17
2.7.1	Gas Phase Intercalation	17
2.7.2	Liquid Phase Intercalation	17
2.7.3	Hydrothermal Intercalation	18
2.7.4	Electrochemical Intercalation	19
2.8	Graphite Exfoliation Methods	20
2.8.1	Mechanical Exfoliation	20
2.8.2	Chemical Exfoliation	21
2.8.3	Chemical Vapour Deposition	22
2.8.4	Electrochemical Exfoliation	23
2.9	Ultrasonication	24
2.10	Summary	24
<b>3</b>	<b>METHODOLOGY AND WORK PLAN</b>	<b>25</b>
3.1	Project Planning	25
3.2	Flowchart	26
3.3	Materials	27
3.4	Experiment Procedures	28
3.4.1	Hydrothermal Intercalation	28
3.4.2	Microwave Exfoliation	33
3.4.3	Fabrication of Supercapacitor	34
3.5	Characterisations	37
3.5.1	Scanning Electron Microscope	37
3.5.2	Field-Emission Scanning Electron Microscope	38
3.5.3	Energy Dispersive X-Ray Spectroscopy	39
3.5.4	X-Ray Diffraction	39
3.5.5	Fourier Transform Infrared Spectroscopy	40

<b>4</b>	<b>RESULTS AND DISCUSSIONS</b>	<b>42</b>
4.1	Comparison of Different Synthesis Methods	42
4.2	Characterisations	42
4.2.1	Scanning Electron Microscope	42
4.2.2	Field-Emission Scanning Electron Microscope	50
4.2.3	Energy Dispersive X-Ray Spectroscopy	52
4.2.4	X-Ray Diffraction	53
4.2.5	Fourier Transform Infrared Spectroscopy	56
4.3	Supercapacitor	58
4.4	Summary	61
<b>5</b>	<b>CONCLUSION AND RECOMMENDATIONS</b>	<b>62</b>
5.1	Conclusion	62
5.2	Recommendations for Future Work	63
	<b>REFERENCES</b>	<b>64</b>
	<b>APPENDICES</b>	<b>70</b>

**LIST OF TABLES**

Table 2.1: Properties of Graphene (Xu, et al., 2017)	8
Table 3.1: List of Chemicals	28
Table 4.1: EDX Elemental Analysis of $FeCl_3 - GIC$ and $FeCl_3 - FLG$ in Wt%	53

**LIST OF FIGURES**

Figure 2.1: Types of Graphite	6
Figure 2.2: GIC (Salvatore, 2017)	6
Figure 2.3: Allotropes of Carbon (Tiwari, et al., 2016)	7
Figure 2.4: GO (Sadyraliev, 2018)	10
Figure 3.1: FYP 1 Gantt Chart	25
Figure 3.2: FYP 2 Gantt Chart	25
Figure 3.3: Project Flowchart	27
Figure 3.4: Rotating Mixtures in Disposable Bottle	28
Figure 3.5: Separation of Mixtures and Grinding Media	29
Figure 3.6: Dried Mixtures	30
Figure 3.7: Clumped Mixtures	30
Figure 3.8: 50 mL Stainless Steel Autoclave	31
Figure 3.9: Heated Mixtures in Teflon Vessel	31
Figure 3.10: Filtration of Mixtures	32
Figure 3.11: $FeCl_3$ – GIC Mixed with N, N-Dimethyl Formamide	32
Figure 3.12: Ultrasonication of Mixtures	33
Figure 3.13: $FeCl_3$ – FLG	33
Figure 3.14: Mixtures of Graphite and $FeCl_3$	34
Figure 3.15: Aluminium Plates Connected to a Copper Wire	35
Figure 3.16: Aluminium Plates with a Layer of $FeCl_3$ – FLG	35
Figure 3.17: Sealed $FeCl_3$ – FLG Supercapacitor	36
Figure 3.18: Setup of Discharging $FeCl_3$ – FLG Supercapacitor	37
Figure 3.19: UTAR SEM	38

Figure 3.20: UTM FESEM	38
Figure 3.21: UTAR XRD	39
Figure 3.22: $FeCl_3$ – FLG XRD Sample	40
Figure 3.23: UTAR FTIR	41
Figure 4.1: Graphite SEM Image at the Magnification of 11 000x	43
Figure 4.2: Graphite SEM Image at the Magnification of 25 000x	43
Figure 4.3: $FeCl_3$ – GIC SEM Image at the Magnification of 9 500x	44
Figure 4.4: $FeCl_3$ – GIC SEM Image at the Magnification of 14 000x	45
Figure 4.5: $FeCl_3$ – GIC SEM Image at the Magnification of 17 000x	46
Figure 4.6: Graphene SEM Image at the Magnification of 27 000x	47
Figure 4.7: Graphene SEM Image at the Magnification of 42 000x	47
Figure 4.8: $FeCl_3$ – FLG SEM Image at the Magnification of 16 000x	48
Figure 4.9: $FeCl_3$ – FLG SEM Image at the Magnification of 23 000x	48
Figure 4.10: $FeCl_3$ – FLG SEM Image at the Magnification of 50 000x	49
Figure 4.11: $FeCl_3$ – FLG SEM Image at the Magnification of 32 000x	49
Figure 4.12: $FeCl_3$ – FLG FESEM Image at the Magnification of 70 000x	50
Figure 4.13: $FeCl_3$ – FLG FESEM Image at the Magnification of 40 000x	51
Figure 4.14: $FeCl_3$ – FLG FESEM Image at the Magnification of 55 000x	51
Figure 4.15: SEM Image of (a) $FeCl_3$ – GIC and (b) $FeCl_3$ – FLG for EDX	52

Figure 4.16: XRD Diffractogram of Graphite and JCPDS Card of Carbon	<b>Error! Bookmark not defined.</b>
Figure 4.17: XRD Diffractogram of $FeCl_3 - GIC$ and JCPDS Cards of Carbon and Iron Oxide	<b>Error! Bookmark not defined.</b>
Figure 4.18: XRD Diffractogram of $FeCl_3 - FLG$ and JCPDS Cards of Carbon, Chlorine and Iron Oxide	<b>Error! Bookmark not defined.</b>
Figure 4.19: $FeCl_3 - GIC$ IR Spectra	57
Figure 4.20: $FeCl_3 - FLG$ IR Spectra	57
Figure 4.21: GO IR Spectra (Rattana, et al., 2012)	58
Figure 4.22: Discharge Curve of Capacitor	59
Figure 4.23: Discharge Curve of $FeCl_3 - GIC$ Supercapacitor	59
Figure 4.24: Discharge Curve of $FeCl_3 - FLG$ Supercapacitor	60
Figure 4.25: Discharge Curves of Normal Capacitor, $FeCl_3 - GIC$ and $FeCl_3 - FLG$ Supercapacitor	61

**LIST OF SYMBOLS / ABBREVIATIONS**

1D	One-Dimensional
2D	Two-Dimensional
3D	Three-Dimensional
AFM	Atomic Force Microscope
At %	Atomic Percentage
CO <sub>2</sub>	Carbon Dioxide
CVD	Chemical Vapour Deposition
EDX	Energy-Dispersive X-Ray Spectroscopy
FeCl <sub>3</sub>	Iron (III) Chloride
FEES	Flexible Electrochemical Energy Storage
FESEM	Field-Emission Scanning Electron Microscope
FLG	Few-Layer Graphene
FTIR	Fourier Transform Infrared Spectroscopy
FYP	Final Year Project
GIC	Graphite Intercalated Compound
GO	Graphene Oxide
ICE	Interlayer Catalytic Exfoliation
JCPDS	Joint Committee on Powder Diffraction Standards
LED	Light Emitting Diode
Li	Lithium
LIB	Lithium-Ion Battery
LIG	Lithium Intercalated Graphite
MIT	Massachusetts Institute of Technology
MLG	Multi-Layer Graphene
SAPCVD	Stationary Atmospheric Pressure Chemical Vapour Deposition
SEM	Scanning Electron Microscope
SLG	Single-layer Graphene
UTM	Universiti Technology Malaysia
Wt %	Weight Percentage
XRD	X-Ray Diffraction

## CHAPTER 1

### INTRODUCTION

#### 1.1 Introduction

In this era of technology, swift development of microprocessor has led to the continuous advancement and miniaturisation of electronic components (Chu, et al., 2018). The concept of graphite intercalated compound (GIC) was developed in the year of 1841, the development of GIC technology had been led by its unique properties of exceptional electrical conductivity and large storage capacity of lithium or hydrogen ions. After the published of GIC in 1841, there has been a great amount of technique developed for the production of GIC (Xu, et al., 2017).

After Novoselov and Geim had successfully isolated a single layer of graphene by using the well-known “scotch-tape method” in the year of 2004 (Lalwani, et al., 2016), researcher started to place strong attention towards GIC, graphene oxide (GO) and graphene owing to their exceptional mechanical, electrical and thermal properties of graphene and its derivative product (Chu, et al., 2018).

As the electronic components nowadays have moved towards the scale of nanometre, the demand for materials that have low mass and excellent electrical properties has been increasing exponentially. The heat dissipation in miniaturised technologies is the most critical and challenging part of the design. The temperature will greatly affect the performance of the circuit, a slight change in temperature will reduce the lifetime of the device. Thus, a material that has low mass and excellent electrical properties such as GIC and few-layer graphene (FLG) are the keys to the development of miniaturised technologies (Ghosh, et al., 2008).

The potential use of graphene as a nanomaterial in utilisation and applications such as sensors, optoelectronics and biomedical is because of their favourable bioactivity and exceptional physicochemical properties. These properties of graphene and its derivatives also developed the abilities in applications for drug delivery, photothermal cancer therapy and human neural stem cell differentiation. In the field of biomedical, graphene can act as an injectable delivery system for repairing certain tissues and drug delivery. It's anti-inflammatory, antibacterial and biocompatibility property is privilege properties that are able to be used on human medical fields (Chaudhuri, et al., 2015).

## **1.2 Importance of the Study**

Nowadays, energy resources are transforming from non-renewable energy such as fossil fuels to renewable energy including biomass, hydroelectricity and solar energy. However, renewable energy is not always available when required. Thus, the advancement of energy storage systems that can store a large amount of energy is critical in overcoming this discrepancy.

Currently, the commonly used method to store energy is through capacitor. However, the usage of capacitor is only limited to small electric appliances such as television, camera and laptop. New technology like electric car requires an energy storage system that is able to store a large amount of energy. Therefore, the breakthrough of limited storage capacity is crucial for new technological possibilities.

GIC and FLG are materials that have high energy storage capacity. Therefore, it has a high potential in the development of large capacity energy storage system. By applying GIC and FLG in current technologies, it can greatly improve the performance of it in term of electrical conductivity, mechanical strength, thermal conductivity and most importantly storage capacity. In this project, GIC and FLG that has high potential in increasing the energy storage capacity of the system will be investigated. The result of this project may greatly affect the evolution of technologies in the future.

## **1.3 Problem Statement**

In order to solve any problem, the first step to it is to identify the problem, then analyse the problem and finally, solve the problem.

GIC, FLG and graphene are the promising materials to improve the storage capacity of the capacitor. FLG can be obtained by ultrasonication GIC in an ultrasonication bath, whereas further ultrasonication of FLG can eventually obtain graphene. Although the performance of graphene is the best, however the synthesis time and power required to obtain graphene from FLG is high, hence, results in high production cost of graphene.

Even though graphene is the best, but the storage capacity of GIC and FLG is excellent too. In this project, GIC and FLG will be used as the materials to fabricate capacitor and compare the performance of the normal capacitor with capacitor that is fabricated using GIC and FLG. The comparison is to determine whether the performance of GIC and FLG is sufficient to solve the problem of limited energy storage capacity of capacitor.

#### 1.4 Aim and Objectives

The aim of this project is to synthesis iron (III) chloride few-layer graphene ( $FeCl_3 - FLG$ ) by interlayer catalytic exfoliation for supercapacitor applications.

In order to accomplish the aim, the listed main objectives as follow are to be accomplished.

- i. To intercalate iron (III) chloride ( $FeCl_3$ ) into the layered structure of graphite and exfoliate it mechanically and chemically through ultrasonication process.
- ii. To determine the characteristics of graphite, synthesised  $FeCl_3 - GIC$  and  $FeCl_3 - FLG$ .
- iii. To determine the characteristics of supercapacitor that is fabricated by synthesised  $FeCl_3 - GIC$  and  $FeCl_3 - FLG$ .

#### 1.5 Scope of Study

The working scope of this project is to synthesis and determine the characteristics of  $FeCl_3 - GIC$  and  $FeCl_3 - FLG$  by using interlayer catalytic exfoliation. First of all,  $FeCl_3$  will be intercalate into the layered structure of graphite to obtain  $FeCl_3 - GIC$ . The synthesised  $FeCl_3 - GIC$  will then ultrasonicate with the aids of solvent to exfoliate into  $FeCl_3 - FLG$ . In order to verify the results of synthesised  $FeCl_3 - GIC$  and  $FeCl_3 - FLG$ , the samples will then characterise by using SEM, FESEM, EDX, XRD and FTIR. The storage capacity of  $FeCl_3 - GIC$  and  $FeCl_3 - FLG$  will be measure by comparing the performance of normal capacitor with  $FeCl_3 - GIC$  supercapacitor and  $FeCl_3 - FLG$  supercapacitor.

#### 1.6 Structure of Thesis

Chapter 1 which is the introduction will cover the brief introduction, importance of study, problem statement, aim and objectives and scope of study of this project.

Chapter 2, literature review will be focus on the background of graphene and its derivatives, applications of graphene, graphite intercalation methods, graphite exfoliation methods and ultrasonication process.

Chapter 3 of this project, which is methodology and work plan will be covering the types of materials used, procedures to synthesis  $FeCl_3 - GIC$ ,  $FeCl_3 - FLG$  and supercapacitors and different characterisation methods.

Chapter 4, results and discussion will be discussing different synthesis methods, characterisation results and performance of supercapacitors.

Chapter 5, which is the conclusion and recommendations will be covering the general conclusion of this study and recommendations for future work.

## CHAPTER 2

### LITERATURE REVIEW

#### 2.1 Introduction

Chapter 2 of this report will be discussing graphite and its derivatives such as GO, GIC and graphene in detail. By inserting intercalant such as  $FeCl_3$  into the layered structure of graphite, GIC can be obtained, further processing of GIC can obtain FLG and single-layer graphene (SLG). Furthermore, the application of graphene, intercalation methods and exfoliation methods of graphite also will be discussed in detail in this chapter.

#### 2.2 Graphite

Graphite is a word that is derived from one of the Greek word, which is “Graphein”. It is a layered structure, where it allows different types of atoms and molecules to insert between the layers of graphite and hence create a compound known as GIC. The process of inserting molecules or atoms between the layered structures of graphite is known as intercalation (Heerden and Badenhorst, 2015).

There are two types of graphite, which is natural graphite and synthetic graphite. Natural graphite is graphite that is formed naturally by the planet Earth, it can be categorised into three types of graphite, which is natural amorphous graphite, natural flakes graphite and high crystalline natural graphite. Natural graphite can then be further categorised into more subcategory, this depends on the impurities, content and particle size of the graphite. Figure 2.1 shows the different types of graphite (Heerden and Badenhorst, 2015).

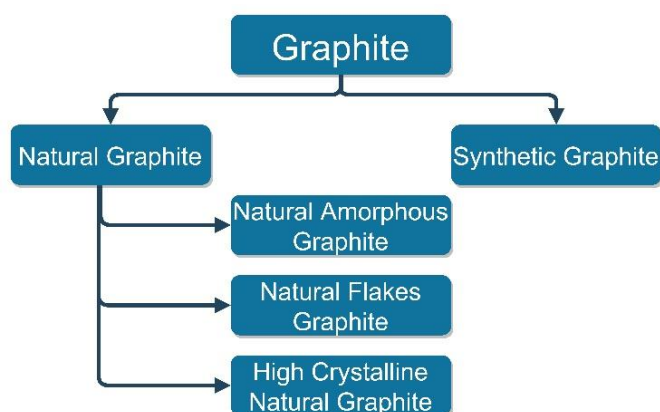


Figure 2.1: Types of Graphite

### 2.3 Graphite Intercalated Compound

GIC is formed by intercalating molecules or atoms between the layers of graphite. It was used as a new type of anode material for LIB due to their exceptional properties. There are numerous journal and article state that the electrical conductivity of GIC is even better than those metal. Electrons can easily transfer through the simple hexagonal lattice and hence conduct electricity effortlessly. Characteristics of GIC make itself as a promising choice of electrode material for LIB (Wang, et al., 2014).

By inserting  $\text{FeCl}_3$  into the interlayer of graphite element,  $\text{FeCl}_3 - \text{GIC}$  is formed.  $\text{FeCl}_3 - \text{GIC}$  is also a potential anode material for rechargeable LIB. Long cycling stability and high storage capacity made it more favourable to be anode material for LIB (Wang, et al., 2014). Figure 2.3 shows the simplified process of GIC formed.

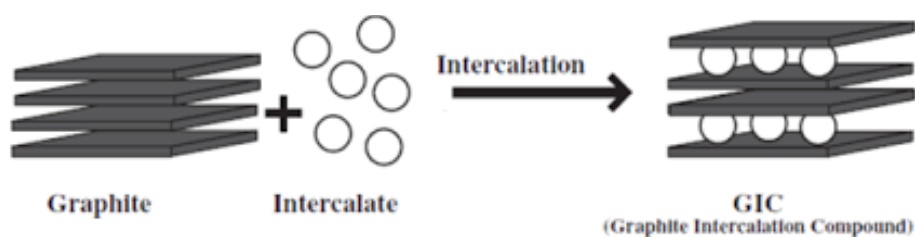


Figure 2.2: GIC (Salvatore, 2017)

### 2.4 Graphene

Diamond, carbynes, carbon nanotube, fullerenes and graphite are different existing allotropic forms of carbon. Graphite, a lamellar semimetal solid, where the most stable form of it is at room temperature. It is formed by weak Van der Waals force that

connecting two-dimensional (2D) graphene layers together and strong covalent bond that forms between the adjacent planes of the carbon atoms that create small carbon to carbon distance. Thus, graphite highly anisotropic properties are the results of strong covalent bond and weak Van der Waals force (Emery, et al., 2009). Figure 2.4 shows the allotropes of carbon.

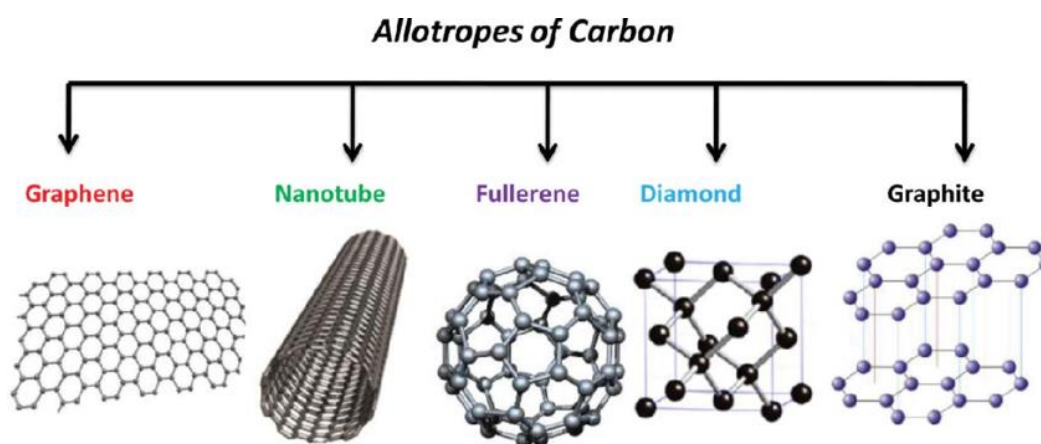


Figure 2.3: Allotropes of Carbon (Tiwari, et al., 2016)

Graphite layered structure allows different atoms or molecules to insert between the layers and hence produce GIC (Heerden and Badenhorst, 2015). Intercalating different species of atoms or molecules into graphene layers will eventually exhibit various excellent chemical and physical properties compared to graphite (Xu, et al., 2017). There are numerous intercalation methods, such as electrochemical intercalation, gas-phase intercalation, liquid-phase and hydrothermal intercalation methods (Heerden and Badenhorst, 2015).

#### 2.4.1 Graphene Properties

Graphene is a layer of graphite, it consists of an atomic layer of carbon atoms which is arranged in a simple honeycomb or hexagonal lattice (Xu, et al., 2017). Even though graphene is just an atomic layer of graphite, it is very stiff and strong compared to most of the metal and non-metal materials (Frank, et al., 2007). Other than graphene extremely high strength, it also has a large surface area, high Young's modulus, large mechanical strength, high charge carrier mobility and high thermal conductivity which are summarised in Table 2.1 as shown below (Xu, et al., 2017).

Table 2.1: Properties of Graphene (Xu, et al., 2017)

<b>Property</b>	<b>Approximated value of graphene</b>
Surface Area ( $m^2/g$ )	2 630
Young's Modulus (GPa)	1 000
Mechanical Strength (GPa)	130
Charge Carrier Mobility ( $cm^2/V \cdot s$ )	200 000
Thermal Conductivity ( $W m /K$ )	5 000

Other than excellent electronic and thermal conductivity properties, graphene also exhibits other extraordinary physical properties. It has been implemented in corrosion inhibitors, polymer composites, biological sensors and chemical sensors. Although it has great potential in enhancing devices, the cost of synthesising large-quantity of high-quality FLG is uneconomical (Whitener and Sheehan, 2014).

Graphene has been recognised as the thinnest matter in the world because it has a thickness of only 0.334 nm. The perfect carbon structure, bonding system and endless repetition of 2D plane structure endow it with various characteristics and extraordinary properties. Thus, it has extensive application potential in semiconductor materials, drug carries, electronic information, photoelectric and energy storage devices (Ren, Rong and Yu, 2018).

#### **2.4.2 Synthesis of graphene**

Since graphene is a single layer of graphite, thus the extraction of graphene from bulk graphite is the simplest and most basic technique to synthesis it (Whitener and Sheehan, 2014).

On the research side, the method to prepare and synthesis high-quality and large-quantity graphene with high efficiency is still in infant stage. Conversely, on the implementation side, the current global supply and demand capacity for graphene is large, industries that are involved in the production and utilisation of graphene is expected to spread globally in this coming few decades. The production of graphene is predicted to be at the magnitude of hundreds and thousands of tons. By the time, high-performance computing materials, structural materials, transparent display materials, supercapacitors and flexible wearable devices will more likely to have a higher potential and greater market (Ren, Rong and Yu, 2018).

In order to produce high-quality and large-quantity of FLG, one of the synthesis methods, which is interlayer catalytic exfoliation (ICE) can be implemented. Adding graphite powder into organic solvents can produce high-quality graphene flakes. It is indeed an environmentally friendly way to synthesis large-quantity of high-quality FLG (Geng, et al., 2013).

Liquid phase exfoliation method is one of the methods that can produce large-quantity of high-quality graphene with relatively low cost. The concept of liquid phase exfoliation method is basically splitting graphite in solution, where graphene layers in graphite are bonded in weak van der Waals forces. There are numerous molecules or atoms that can be intercalated between graphene layers and have the ability to expand the interlayer distance. The examples of intercalant are lithium, potassium,  $FeCl_3$ , hydrate salt and sulphur (Yoon, et al., 2015). Large thickness of GIC will affect the storage performance, thinner layer of GIC, such as FLG is highly preferable as it exhibits better electrical and thermal conductivity (Qi, et al., 2015).

## 2.5 Graphene Oxide

A derivative of graphene which had been highly oxidised can be defined as GO. It composes of several functional groups like epoxy, carbonyl, carboxyl and hydroxyl functional group. All of the oxygen-containing groups can be found on the bottom and edges of the graphene itself (Galpaya, 2015). From the structure of GO, it can be observed that it is almost similar to graphene, differing only the oxygen-containing functional groups that contain in the GO, which separate the distance between the layered structures of graphite (Lopez, et al., 2016). The oxygen-containing functional groups are the reason that makes the multifunctional material highly attracted to GO. It has been extensively used in various application as GO can freely alter with various functional groups (Galpaya, 2015). Figure 2.4 shows graphene oxide with different oxygen-containing functional groups.

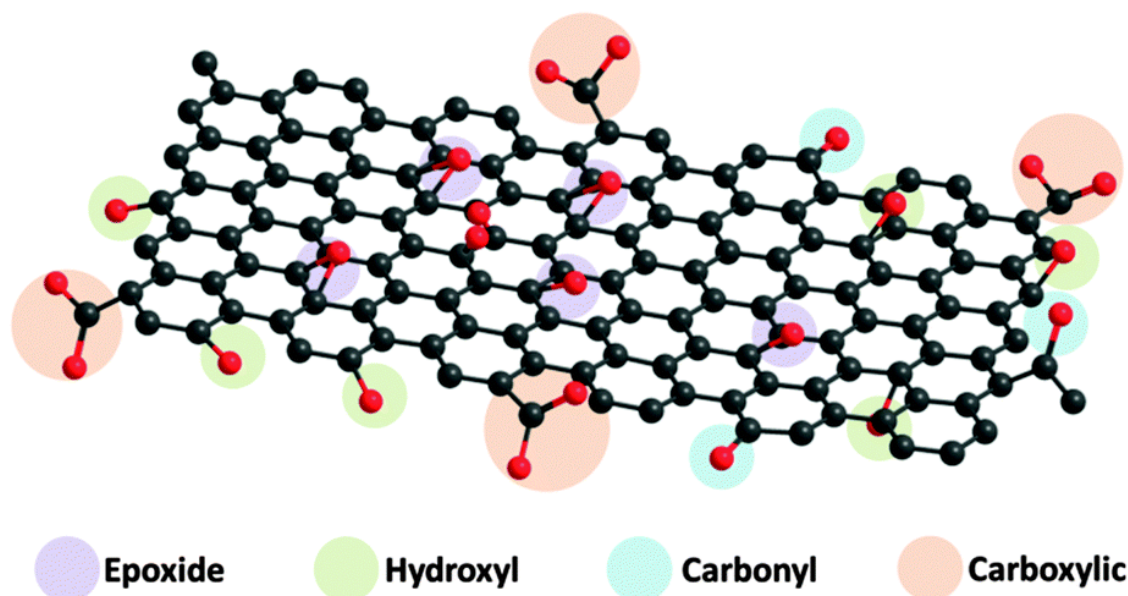


Figure 2.4: GO (Sadyraliev, 2018)

## 2.6 Applications of Graphene

### 2.6.1 Graphene Bulb

In current development, light-emitting diode (LED) is the bottleneck stage of the evolution of the light bulb. Although LED consumes low power, coating a layer of graphene at the outside of LED can highly reduce the energy consumption of the bulb. This development had led the electronic industries to a brighter and promising direction (Ren, Rong and Yu, 2018).

According to Ren, Rong and Yu (2018), the University of Manchester developed graphene bulb that is able to increase LED life expectancy and performance through the coating of graphene on the LED. Graphene bulbs which are stronger compared to LED also have lower prices than LED (Ren, Rong and Yu, 2018).

The graphene layer that coated on the outer layer of LED has granted LED to have higher conductivity, it also allows graphene bulbs to have a higher strain and simultaneously reducing its power consumption by 10 % (Ren, Rong and Yu, 2018).

Lai, et al. (2017) also successfully fabricate graphene bulb by coating a layer of graphite based ink to circuit boards. The filaments that were used to synthesis graphene bulb were graphene filament. It was then found out that by applying this method, the graphene bulb will have a greater advantage in energy consumption (Lai, et al., 2017).

### **2.6.2 Graphene Superconductor**

In the year 1991, it was found that the resistance of mercury at a very low temperature will be almost zero and thus, in a superconducting state. Thence, the research on superconductors increases exponentially. As for graphene, there are 2 ways to achieve the superconducting state. The first method is easier to be achieved, which is to increase the temperature limit of it. The second method is to discover a new technique to merge the matrix with a dopant for stabilising and enhancing its superconductivity (Ren, Rong and Yu, 2018).

Columbia University successfully synthesised graphene that has a high potential to achieve superconductivity by doping lithium ion to graphite and cool it down to  $-267.25\text{ }^{\circ}\text{C}$  (Ren, Rong and Yu, 2018). Bernardo, et al. (2017) from University of Cambridge mixed praseodymium-cerium oxide with graphene, which results in the activation of potential superconductivity of graphene (Bernardo, et al., 2017).

Furthermore, flexible graphite superconducting fibres were successfully synthesised by Liu, et al. (2017) by intercalating calcium into graphene fibres. The results of the calcium intercalated graphite fibres showed that when it is at  $-262.15\text{ }^{\circ}\text{C}$ , it exhibits a superconducting phase transition. It also showed similar properties to Niobium-Titanium superconducting wire. The excellent properties of Calcium intercalated graphite fibres such as scalability and lightweight made it a promising material for lightweight superconducting line (Liu, et al., 2017).

Dong, et al. (2016) from Tsinghua University fabricated breathable portable superconductor by using layered electrodes that have high flexibility. The base of the flexible material is made out of a permeable mesh layer, while electrochemical active electrodes are deposited by manganese dioxide and carbon nanotubes. The active electrode has incredible properties such as high cyclic performance, flexibility and also high ratio capacity. These properties have made a relatively strong impact on wearable and portable electronic devices, as it is flexible enough to twist, shape and fold (Dong, et al., 2016).

### **2.6.3 Graphene Chip**

The raw material for an integrated circuit has been silicon for the past few decades as it has a negative temperature coefficient. Which mean that as the temperature of the integrated circuit increase, its resistance will decrease. However, it also has a critical disadvantage of lack of space for advancement. Fortunately, with the graphene

technology, integrated circuit industry is facing a transformation (Ren, Rong and Yu, 2018).

Storage and transfer of data by applying the technology of graphene have been developed by the researcher at Massachusetts Institute of Technology (MIT). Graphene technology able to increase the calculation speed of an integrated circuit by millions of times, thus making the microchip has a high level of computing power (Ren, Rong and Yu, 2018).

According to El-Kady and Kaner (2013), graphene miniature supercapacitor is the combination of around 100 micro-scale supercapacitors on an integrated circuit by direct laser writing. In the fabrication results, it showed that graphene increased the power density, storage rate and charge storage capacity of any supercapacitors (El-Kady and Kaner, 2013).

Alymov, et al. (2016) fabricated bilayer graphene by the adhesion of two-layer graphene. It was then used to construct an extremely low energy consumption graphene transistor, an astonishing processing speed of 100 GHz was successfully produced. There are also a large number of experiments has been conducted to prove the graphene transistors require a very little amount of energy. The graphene chip requires very little amount of energy, therefore, the amount of heat produced is also very small. Less amount of dissipated heat also means that the graphene chips does not need a cooling system to reduce its temperature. This also solves the problem of graphene chip destroyed by the excess heat as well (Alymov, et al., 2016).

#### **2.6.4 Drug Carrier**

The researcher had developed an injectable graphene delivery system for certain tissue repairment. Different groups of researcher also tested graphene with mammalian cells due to its anti-inflammatory, antibacterial and biocompatibility property. Graphene also showed accelerated and controlled differentiation of human osteogenic stem cell. All of these unveil that graphene is extraordinary biocompatibility based material for biomedical applications (Chaudhuri, et al., 2015).

Yang, et al. (2011) utilising multi-functionalised GO to fabricate a dual-targeting drug delivery, where its drug release system is controlled by a pH-sensitive control. The aim of this project is to improve target drug delivery. At the end of the projects, the results show that multi-functionalised GO dual-targeting drug delivery

has the potential to be utilised in the application of controlled release (Yang, et al., 2011).

### **2.6.5 Hydrogen Storage Materials**

The extraordinary gas absorption characteristics of graphene have increased its potential in becoming a new type of material in storing hydrogen. Graphene can absorb hydrogen quickly at room temperature at the same time showing high stability (Ren, Rong and Yu, 2018).

Shayeganfar and Shahsavari (2016) had introduced pillar boron nitride-graphene which is a high-performance material that can store hydrogen. It is a three-dimensional (3D) structure of hydrogen storage material that is formed by the combination of graphene and oxygen-doped boron nitride nanotubes. This technology showed that it can carry 11.6 % weight hydrogens. Besides, the capacity to store hydrogen can be reached to 60 g/l. When it is at 160.6 °C, its capacity to store hydrogen can be increased to 14.77 % and can withstand up to 1500 times of charging cycle. All of the excellent results showed that it can greatly assist in the field of hydrogen electric vehicle in the coming future (Shayeganfar and Shahsavari, 2016).

Kumar, et al. 2015 achieved carbon monoxide oxidation multi-functionalities and ultrahigh hydrogen storage by introducing palladium-embedded porous graphene and nanohole-structured. Poly-carbon Nano-palladium will create a pore-like structure through the substrate plane structure of graphene and microwave reaction. It shows the defective graphene structure has a hydrogen storage capacity of 5.4 % under the pressure of 7.5 MPa. It also can be implemented in catalytic activity, molecular absorption and electrochemical storage (Kumar, et al., 2015).

According to Zhou, Szpunar and Cui (2016) nickel nanoparticle with the size of 10 nm was spread uniformly on graphene substrate to fabricate graphene-based nickel composite for the use of storing hydrogen. The system exhibits an impressive property such as low activation temperature, high gravimetric density and ambient conditions for hydrogen release when the pressure of hydrogen is at 1 bar and it is under atmospheric pressure and room temperature. There are a large amount of experiments that can prove the capacity of the system to store hydrogen is 0.14 wt. %. Whereas, if the pressure of hydrogen was increased to 60 bar and the temperature of the system is in the range of 150 °C to 250 °C, the storing capacity will be increased to 1.18 wt. % (Zhou, Szpunar and Cui, 2016).

Moreover, Ozturk, Baykasoglu and Kirca, (2016) had fabricated a new type of material to keep hydrogen. Sandwiched graphene-fullerene is a nano-composite material that has a large surface area and exhibits high stability when the temperature is at  $-196.2\text{ }^{\circ}\text{C}$ . When the pressure of hydrogen is at 1 bar, the sandwiched structure can store hydrogen up to 3.83 %. If lithium is used as a dopant with a lithium-carbon ratio of 1:8, the capacity to store hydrogen can reach 5 %. All collected results and data showed that this sandwiched structure hydrogen storage capacity is full of possibility (Ozturk, Baykasoglu and Kirca, 2016).

### **2.6.6 Graphene Battery**

As current science and technology develop, the demand for LIB with higher energy density, better performance cycle and lower manufacturing cost have become higher and obvious. Thus, the need to develop graphene energy storage device has become a hot topic among researchers and scientists (Ren, Rong and Yu, 2018).

Furthermore, Raji, et al. (2017) used carbon nanotubes mixtures and graphene fabricated rechargeable LIB, where the cathode of the graphene battery is made out of carbon nanotube and graphene that is coated with lithium metal. The results of it showed that the storage capacity of the LIB is three times higher than the normal commercial LIB. (Raji, et al., 2017).

On the other hand, Abouimrane, et al. (2010) had developed a technique to fabricate a negative electrode of LIB without using any polymer additives and binders. The non-annealed graphene is the only raw material that was used to fabricate the additive-free LIB, it exhibits rapid discharge properties, excellent cyclability and high battery capacity, which will greatly boost the performance of anode in LIB (Abouimrane, et al., 2010).

Hu, Li and Chen (2017) created a liquid-lithium-carbon dioxide (Liquid-Li-CO<sub>2</sub>) battery, its energy can be generated by using CO<sub>2</sub> for the use of wearable electronic devices. Liquid-free electrolytes also can use the generated energy because it is more reliable and safer. The Liquid-Li-CO<sub>2</sub> battery can operate for 220 hours under the conditions of  $55\text{ }^{\circ}\text{C}$  and at a different bending angle of  $0^{\circ}$  to  $360^{\circ}$  (Hu, Li and Chen, 2017).

In addition, Qie, et al. (2017) created a new type of cathode catalyst material by doping porous graphene with nitrogen and boron. This carbon-based catalyst had broadened the field of long-term Li-air batteries by the excellent properties of Li-CO<sub>2</sub>

battery such as high current density, high reversibility, long-term cycling stability, low polarisation and outstanding performance rate (Qie, et al., 2017).

Son, et al. (2017) had coated graphene ball onto nickel-rich layered cathode materials. The uniform coating of graphene ball strengthens the properties of the cathode materials such as enhancing the charging performance, thermal stability and cyclic stability of the cathode materials (Son, et al., 2017).

### **2.6.7 Graphene Supercapacitor**

A supercapacitor is an emerging new technology that has better energy storing capacity compared to conventional battery and capacitor. It is green and one of the most promising devices that can store physical energy (Ren, Rong and Yu, 2018). According to Ali, et al. (2015), the properties of supercapacitor can be improved by graphene oxide nanosheet (Ali, et al., 2015). Xiao, et al. (2017) also fabricated a high-energy micro-supercapacitors, it showed extraordinary conductivity, uniformity, structural integration and flexibility (Xiao, et al., 2017).

Feng, et al. (2017) stated that the developed high energy density flexible solid-state supercapacitor showed outstanding energy density, specific capacitance and rate capability. The specific capacitance of the supercapacitor is stated to maintain above 85 % after 10 000 cycles. The capacitor also proves that it has excellent mechanical flexural and electrochemical properties as well. From all the above research results, it can be concluded that the breakthrough of this technology is going to make a significant contribution to future flexible energy storage devices (Feng, et al., 2017).

### **2.6.8 Graphene Wearable Functional Devices**

Currently, we are entering a brand new era, where most of the devices and equipment are wearable and flexible. The emerging of flexible electrochemical energy storage (FEES) technology had brought a large amount of attention towards the advancement of flexible wearable electronic devices (Ren, Rong and Yu, 2018).

Wen, Li and Cheng (2016) had discussed the utilisation of graphene and carbon nanotubes in FEES in detail. The major difficulty that was faced in fabricating FEES device is to achieve both extensibility and bendability at the same time, however, by introducing carbon nanotubes and graphene into FEES devices can easily resolve the complication. Although the FEES device is under extreme conditions, the electrochemical properties and the limit of the bending radius are still in good

conditions. This is all because of the extraordinary mechanical properties and special structure of carbon nanotubes and graphene. It also can be implemented on three different types of tensile structures effortlessly due to its unique one-dimensional (1D) and 2D structure (Wen, Li and Cheng, 2016).

Nardecchia, et al. (2012) used graphene foam, carbon nanotube and carbon aerogel to fabricate a large 3D compressible devices. The holey-structure of graphene and carbon nanotubes can remain its outstanding electrical conductivity under its full compression is all because of its excellent compressibility and self-connectivity (Nardecchia, et al., 2012).

Gaikwad, et al. (2011) had developed a zinc-carbon battery which has a benefit of stable discharge capacity and low manufacturing cost. The major materials that used to fabricate the flexible conductive collector are carbon nanotubes and graphene, the materials also used as the additive for cathode and anode materials of the battery (Gaikwad, et al., 2011).

Oh, et al. (2016) used the extraordinary properties of carbon nanotubes and graphene to develop organic transistors which are intrinsically healable and stretchable. The organic transistors were applied on the human arm for testing, it showed that the organic transistor can retain its high charge-carrier mobility even it undergone a series of regular movement (Oh, et al., 2016).

Tao, et al. (2017) from Tsinghua University used graphene technology to fabricate intelligent artificial throat, it uses graphene to emit and receives sound by utilising graphene sound effect and piezoresistive effect, respectively. Material that used to make artificial larynx that can emit sound wave between 100 Hz to 40 kHz are holey-structure graphene. The reasons that holey-structure graphene was utilised is because it has a low heat capacity rate and high thermal conductivity. The holey-structure of graphene able to detect the change in vibration precisely when it is located in the throat and receive sound wave through piezoresistive effect (Tao, et al., 2017).

Other than that, Tian, et al. (2014) also developed a flexible headset by applying a one-step laser scribing technology on graphene. This new type of flexible headset is able to detect a minor change in vibration compared to the conventional magnetic headset. It also has a flatter and wider output compared to the conventional headset. It had been reported that this new technology is able to communicate with the animal as the animal sensitivity towards the ultrasonic band are higher compared to human (Tian, et al., 2014).

## 2.7 Graphite Intercalation Methods

There are numerous intercalation methods such as gas phase, liquid phase, hydrothermal, electrochemical and ternary intercalation methods to intercalate different species of intercalant into the layer of graphite. Intercalation of intercalant into the layered structure of graphite may enhance the properties of graphite and at the same time exfoliate graphite into GIC. (Heerden and Badenhorst, 2015).

### 2.7.1 Gas Phase Intercalation

According to Shornikova, et al. (2006), Stage 1 GIC can be obtained by applying a temperature range between 300 °C to 360 °C for 4 hours to 24 hours in a two-zone ampoule, where one of the sides was placed with graphite and another side is  $FeCl_3$ . By applying different heating temperature and reaction time, different stage of  $FeCl_3 - GIC$  can be obtained. If the heating temperature of graphite and  $FeCl_3$  are 310 °C and 300 °C, respectively, with a reaction time of 18 – 25 hours, stage 1  $FeCl_3 - GIC$  can be obtained. Besides, Stage 2  $FeCl_3 - GIC$  can be obtained by heating graphite and  $FeCl_3$  at 360 °C and 300 °C, respectively, with a reaction time of 3 – 25 hours. It can be observed that as the reaction time increase, the amount of chloride intercalated into graphite increases as well (Shornikova, et al., 2006).

Heerden and Badenhorst (2015) also synthesised  $FeCl_3 - GIC$  by using gas phase intercalation method. They intercalated graphite using anhydrous  $FeCl_3$ . The mixture was dried in an oven at 50 °C for 2 hours and instantly transferred to a perfectly sealed reaction cylinder. The reaction cylinder was then heated at 300 °C for 25 hours. The mixture product was then placed into hydrochloric acid and rinsed with deionised water to get  $FeCl_3 - GIC$  (Heerden and Badenhorst, 2015).

### 2.7.2 Liquid Phase Intercalation

There are many liquid phase intercalation methods to intercalate graphite, such as the Staudenmaier method, the Brodie method, the Hofman's method and the Hummers method. Among all the methods, the most common liquid phase intercalation method is the Staudenmaier method. This method uses oxidisers like nitric acid and potassium chlorate to oxidise graphite then uses a strong acid such as sulphuric acid to intercalate into graphite forming GIC (Heerden and Badenhorst, 2015).

The Brodie method is the modifications of the Staudenmaier method. Both of the methods use the same procedure to synthesis GIC, except the ratio of oxidiser and intercalant is different. The Hofman's method and the Hummers method were the modification of Staudenmaier method as well. However, instead of using nitric acid and potassium chlorate as an oxidiser, the Hofman's method and the Hummers method used sodium nitrate and potassium permanganate as an oxidiser, respectively (Heerden and Badenhorst, 2015).

On the other hand, there are also modified Hummers method. Basically, this method is the combination of the Staudenmaier and the Hummers methods. It used concentrated sulphuric acid and concentrated nitric acid to mix with potassium permanganate and graphite. The mixture was kept at ambient temperature and under continuous stirring for 10 minutes. After 10 minutes, it was left for an hour and immersed in distilled water for 2 hours. Next, it was filtered and washed with deionised water until a neutral pH value was reached, it was then dried in a conventional oven at 60 °C (Heerden and Badenhorst, 2015).

### **2.7.3 Hydrothermal Intercalation**

Hydrothermal intercalation is a method that both expansion and intercalation take place under microwave irradiation. Natural flake graphite is oxidised by potassium permanganate and intercalated by nitric acid, which also promotes oxidation in the process. After the mixing process, the mixture was placed into an oven to irradiate for 1 minute. Other than potassium permanganate and nitric acid, hydrogen peroxide and sulphuric acid can also be used as oxidiser and intercalant, respectively for synthesising expanded GIC by hydrothermal intercalation method (Heerden and Badenhorst, 2015).

Wei, et al (2008) stated that the maximum expanded volume that can be obtained was by mixing natural flake graphite, nitric acid and potassium permanganate at a weight ratio of 1:2:1. Wei, et al (2008) also stated that an opened graphite and oxidised of the edge of graphite indicating that it was successful intercalation. Thus, potassium permanganate that acts as a strong oxidising agent with high oxidation rate is required to achieve higher expansion. The amount and properties of oxidiser used in the reaction will greatly affect the expansion volume of the graphite (Wei, et al., 2008).

Furthermore, a nitric acid that was used in the reaction not only act as an intercalating agent, it also functions as an acid which assists in the oxidation of

potassium permanganate. As the amount of nitric acid in the reaction was increased, more nitric acid was intercalated into graphite and eventually results in higher expansion ratio (Wei, et al., 2008).

According to Zhu, et al. (2003) mixture of natural graphite flake with hydrogen peroxide, copper (II) chloride,  $FeCl_3$  hexahydrate and concentrated sulphuric acid in a predetermined ratio were performed. The mixture was placed into a hydrothermal autoclave and heated at a temperature between 70 °C and 180 °C for 4 to 15 hours. After heating, it was filtered and washed with deionised water until a neutral pH value was reached, it was then dried in a conventional oven at 60 °C. The oxidiser is essential in the reaction because intercalation will never take place without an oxidiser. In the reaction, hydrogen peroxide function as oxidiser reacted with concentrated sulphuric acid to enhance the intercalation process. In this reaction, the optimum reaction temperature and time are 120 °C and 12 hours, respectively (Zhu, et al., 2003).

#### **2.7.4 Electrochemical Intercalation**

According to Kang, et al (2002), electrochemical intercalation of graphite is done by sealing 600 g of natural graphite in a net polypropylene bag. The sealed bag then dipped into 93 % sulphuric acid. An anode which is made out of stainless steel plate with a dimension of 40 x 50 cm<sup>2</sup> was placed in the middle of the polypropylene bag. In another hand, the cathode is represented by using two stainless steel plate with the same dimension that was used as the anode. Both the cathode and anode were maintained parallel to each other to guarantee the reaction are uniform. The synthesised sulphuric acid- GIC were rinsed with deionised water until a pH value of 4 to 5 was reached. The products were then dried in a conventional oven at a temperature of 110 °C for 2 hours. After the drying process, the compounds were quickly heated at 1000 °C in a muffle furnace to get an end product of expanded graphite (Kang, et al., 2002).

Similar electrochemical intercalation method was also used by Shornikova, et al. (2006) to synthesis co-intercalation of  $FeCl_3$  and acetic acid into graphite. This was synthesised by using graphite that underwent electrochemical treatment with  $FeCl_3$  and acetic acid. It also stated that electrical conductivity can be increased by adding a suitable amount of hydrochloric acid into the electrolyte. End products of stage 3 and stage 5 GIC were acquired at the end of the reaction. Shornikova, et al (2006)

concluded that there were a number of mass losses in the reaction. The mass loss may be  $FeCl_3$  oxidation, de-intercalation and decomposition of solvent (Shornikova, et al., 2006).

## **2.8 Graphite Exfoliation Methods**

Graphite is a layered structure of graphene which consists of 2D plane that is stacked together to form a 3D structure of graphite element. An important step has been made by the researchers to discover that the layered crystal structure can be separated into few-layer and even a layer. Since then, numerous methods have been discovered to exfoliate the layered graphite structure (Nicholosi, et al., 2013).

### **2.8.1 Mechanical Exfoliation**

Mechanical exfoliation is the first recognised top-down approach to synthesis graphene (Alwarappan and Pillai, 2011). This is a method that is useful in separating sheets of the layered 2D structure into few-layer and even single-layer structure. This method also commonly be known as the scotch tape method. It was performed by simply using an adhesive tape to acquired graphene and this technique was repeated to get a fewer layer. After researcher have been adopted this method for many years, Novoselov, et al. (2004) realise that this thin flakes can be further cleaved into thinner graphene, such as FLG and SLG (Whitener and Sheehan, 2014).

The breakthrough in this method allowed Novoselov, et al. (2004) to perform an experiment that could demonstrate the unique properties of graphene. It is a straightforward synthesis method that does not require any specialised equipment. A small piece of adhesive tape is enough to peel off the surface of graphite. FLG and SLG can be obtained by using a clean adhesive tape to stick it to the first piece of tape. Thinner flakes can be obtained by just peeling off both of the tapes. Thinner sheets of graphite can be obtained by simply increase the iteration of this process as many times as desired (Whitener and Sheehan, 2014).

Although there are numerous methods to synthesis graphene, mechanical cleavage still a popular and favourable method for graphene production and researcher to use for demonstration and educational purpose. This is because this method can acquire high-quality graphene with surfaces that are extremely clean (Whitener and Sheehan, 2014).

Annett and Cross (2016) synthesised high-quality SLG by tearing monolayer graphene using thermodynamics force. It is a synthesising method that is able to obtain large-quantity of graphene with a physical method (Annett and Cross, 2016). Teng, et al (2017) had succeeded to synthesis graphene paper that is highly conductive and also successfully synthesised a high-density, high-quality, large volume and surface free graphene by using ball-mill to exfoliate graphene (Teng, et al., 2017).

### **2.8.2 Chemical Exfoliation**

Chemical exfoliation is similar to mechanical exfoliation. It intercalates alkali metals within the layered structure of graphite in order to separate FLG out of graphite. Due to the different stoichiometric ratios of graphite to alkali metals, alkali metals is one of the elements in the periodic table that is able to easily intercalate into the layered structure of graphite. One of the main advantages is that the ionic radii of alkali metals are smaller compared to the distance between the layers of graphite, therefore, it can fit between the interlayer effortlessly (Alwarappan and Pillai, 2011).

Chemical exfoliation is a scalable, sustainable and versatile way to fabricate FLG and SLG. Most of the form of the carbon elements are absolutely insoluble under normal laboratory conditions. This has been the major obstruction for researchers that are studying carbon nanotubes because nanotubes tend to clump and cluster together and cannot dissolve by any commonly available solvents (Whitener and Sheehan, 2014).

Normally chemical exfoliation involved three main steps. The first step is the mixture of graphite into solvent or surfactants. The mixture will then undergo sonication to exfoliate the graphite into layers or layer of graphene. Finally, the exfoliated graphite will be separated from the non-exfoliated graphite (Papageorgiou, Kinloch and Young, 2017).

There are generally two approaches for chemical exfoliation. In the first approach, graphite is mixed with a surfactant and water. The mixture will then undergo sonication. The hydrophobic graphite will interact with the hydrophobic group of the surfactant, whereas the individual graphite in the solution will be stabilised by the hydrophilic group of the surfactant (Whitener and Sheehan, 2014).

The second approach was to directly sonicate the graphite in a solvent, where it has a surface energy that is similar to the carbonaceous material. This method can decrease the energy that is obstructing the researchers to isolate SLG from graphite

layered crystal structure and allow a small portion of weakly dissolved graphite to persist in the solution (Whitener and Sheehan, 2014).

According to Hernandez, et al. (2008), FLG has been produced by sonicating graphite powder in N-methyl pyrrolidone and using centrifugation technique to remove large pieces of non-exfoliated graphite. In over a period of weeks to months, the FLG that produced showed astonishing stability toward aggregation (Hernandez, et al., 2008).

According to Paton, et al. (2014), it is not just sonication that can exfoliate the layered structure, high shear forces can also be used to exfoliate layered graphite structure on 100 Litre scale. The critical shear rate can be applied by the simple kitchen instrument such as conventional kitchen blenders. The lateral size was found to be in the range of 300 nm to 800 nm with the number of layers of less than 10 layers (Paton, et al., 2014).

Dimiev, et al. (2016) also produced graphene nanoplatelets within a time duration of three to four hours at room temperature. The yield that converts from graphite layered structure to graphite nanoplatelets were almost 100 % (Dimiev, et al., 2016). By judging the equipment and knowledge of industrial nowadays, chemical exfoliation may be the most suitable choice for synthesising large-quantity of high-quality graphene (Papageorgiou, Kinloch and Young, 2017).

### **2.8.3 Chemical Vapour Deposition**

Chemical Vapour Deposition (CVD) is a technique where a thin film of liquid or vapour reactant were built on the surface of the substrate. This chemical reaction is performed in a reaction chamber (Ren, Rong and Yu, 2018). There is also various type of CVD methods, such as thermal CVD, plasma-enhanced CVD, hot wall CVD and cold wall CVD. (Papageorgiou, Kinloch and Young, 2017)

A large area of graphene can be obtained by placing a metal in a reaction chamber and exposed to different hydrocarbon precursors at a relatively high temperature. The types of precursors that was exposed to can be divided into two types, liquid precursors such as pentane or hexane and gaseous hydrocarbons like ethylene, acetylene and methane. (Papageorgiou, Kinloch and Young, 2017).

CVD is a fabrication method that is widely used in the production of semiconductor sheet, it is also one of the ways to fabricate large-quantity, high-purity and high-quality graphene. On the other hand, having a slow growth rate is one of the

major disadvantages that is limiting the development of graphene in this field (Ren, Rong and Yu, 2018).

According to Xu, et al. (2016), a copper foil catalyst was placed on the oxide substrate, the distance between the oxide substrate and the copper foil catalyst are 15  $\mu\text{m}$ . Oxygen was supplied to the copper foil catalyst continuously through the oxide substrate. By continuously supply oxygen to the copper foil catalyst can significantly reduce the energy barrier of carbon material deposition (Xu, et al., 2016).

Zheng, et al. (2013) improved the quality and growing speed of graphene by sonicating the substrate. The Raman and Atomic Force Microscope (AFM) results showed that the defects and folds of the substrate that had undergone ultrasonic treatment had significantly reduced. In addition, the growth rate of the ultrasound-treated target substrates also increases substantially compared with the substrate that has not been ultrasound-treated (Zheng, et al., 2013).

Based on the concept of molecular thermal motion, Xu, et al. (2017) had established stationary-atmospheric-pressure CVD (SAPCVD) system. It is a system that can accomplish a quick fabrication of high-quality graphene. By comparing the results of SAPCVD with traditional CVD, SAPCVD has characteristics of uniform optics, batch quantization and low cost (Xu, et al., 2017).

#### **2.8.4 Electrochemical Exfoliation**

Electrochemical exfoliation is a process that involved the use of electrolyte and electric current. The function of the electrolyte is used to conduct electricity, whereas an electric current is used to consume the graphite electrode when synthesising graphene. This exfoliation process will occur through cathodic reaction or anodic oxidation, where the based material of the electrodes must be graphite-based (Papageorgiou, Kinloch and Young, 2017).

In order to synthesis high-quality FLG that is used for energy and optical application, cathodic reaction is more suitable and recommended. Whereas anodic oxidation is more likely to be published as literature because this method has a low yield, synthesis several graphene layers and resembles GO at its oxidation state compared to pristine SLG (Papageorgiou, Kinloch and Young, 2017).

Electrochemical exfoliation is easier to operate and control because this method is a single step process, where it only took minutes or hours to complete the

exfoliation. Compared to other methods that required a longer time to prepare and stabilise the final products (Papageorgiou, Kinloch and Young, 2017).

However, the main disadvantage of these methods is having expensive ionic liquids in some of the electrochemical exfoliation methods. The probability that crumpled morphology of graphene may produce also limiting the application of this method (Papageorgiou, Kinloch and Young, 2017).

## **2.9 Ultrasonication**

Sonication is a process of utilising sound energy to agitate the particles of the desired objects. Due to the ultrasonic frequencies of more than 20 kHz was applied by the sonication device, sonication process also can be known as ultrasonication as well. Ultrasonication process is done by devices such as ultrasonication bath and ultrasonication probe. Ultrasonication process is used to disperse, mill, extract, disintegrate, emulsify, de-agglomerate, lysis, homogenise and exfoliate the desired samples. It is used to break down and exfoliate the  $\text{FeCl}_3$ -GIC to get  $\text{FeCl}_3$ -FLG and  $\text{FeCl}_3$ -SLG in this project. This is to reveal the surfaces within the graphite layered structures and to examine the properties of the products. In this project, the products that already undergone the ultrasonication process is known as exfoliated  $\text{FeCl}_3$ -GIC, which is  $\text{FeCl}_3$ -FLG or  $\text{FeCl}_3$ -SLG (Heerden and Badenhorst, 2015).

## **2.10 Summary**

In short, the extraordinary properties of graphene has made it have high potential in various fields such as biomedical, engineering, micromachine, electrical vehicle and electronics fields. Among all the intercalation methods, hydrothermal intercalation is one of the most suitable methods that can be implemented in this project, because it is the combination of both expansion and intercalation process. Thus, it can enhance the intercalation process. Besides, chemical exfoliation was utilised in this project to separate GIC into FLG and SLG because it is more economical and simple compared to other methods.

## CHAPTER 3

### METHODOLOGY AND WORK PLAN

#### 3.1 Project Planning

Project planning is an important approach to plan the actions that need to be done, as it can clearly identify the estimated duration of the activity. Figure 3.1 and Figure 3.2 shows the project planning Gantt chart for Final Year Project (FYP) 1 and FYP 2, respectively. In the below Gantt chart, it displays the name of the task, duration of the task, starts and end date. For example, according to Figure 3.1, the first task is title selection, which has a duration of 7 days including weekends. This task starts on 28<sup>th</sup> May and ends on 4<sup>th</sup> June 2018. Task 2, which is the literature review will start as soon as task 1 has been completed.



Figure 3.1: FYP 1 Gantt Chart

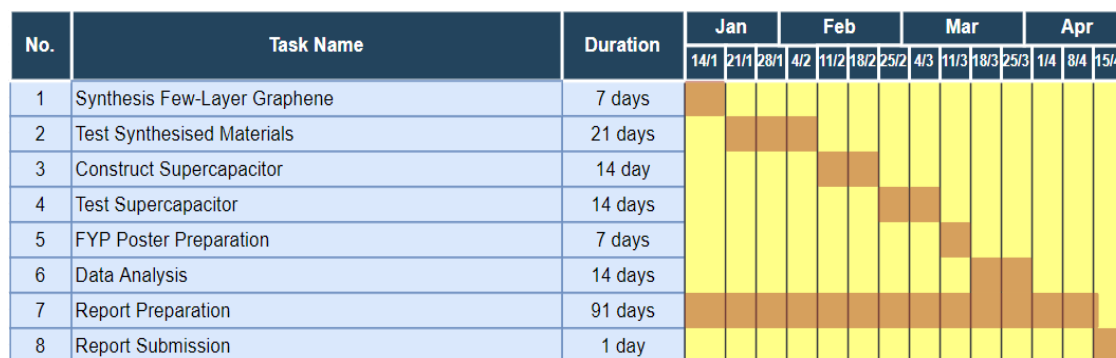


Figure 3.2: FYP 2 Gantt Chart

### **3.2 Flowchart**

In order to complete the FYP, a flowchart that shows in Figure 3.3 represents the expected flow of processes that need to be accomplished was plotted.

The FYP was started with an understanding of the topic. Understanding of topic can ensure that the project that is going to conduct is in the range of the topic. Next will be the study and analysis of other researchers and scientist's works. There are many methods that were proposed by researchers that can eventually accomplish the aim and objectives of this project, however, the suitable and best method will be chosen to complete this project because of limited time and resources.

Furthermore, determine the experimental parameters such as the limitation and scope can assist in experimental planning and setup. Preliminary testing of the selected method can begin as soon as the planning and setup of the experiment are done.

Once the aim and objectives of the project can be established by the results of the preliminary testing, the actual experiment can be started and the gathering of data and results can be performed as well. The collected data and results will be interpreted and analysed, it will be discussed in the report of FYP. Recommendation on the project will be given for future study or improvement of the project too. Finally, the results and findings of this project will be presented to the supervisor and related personnel.

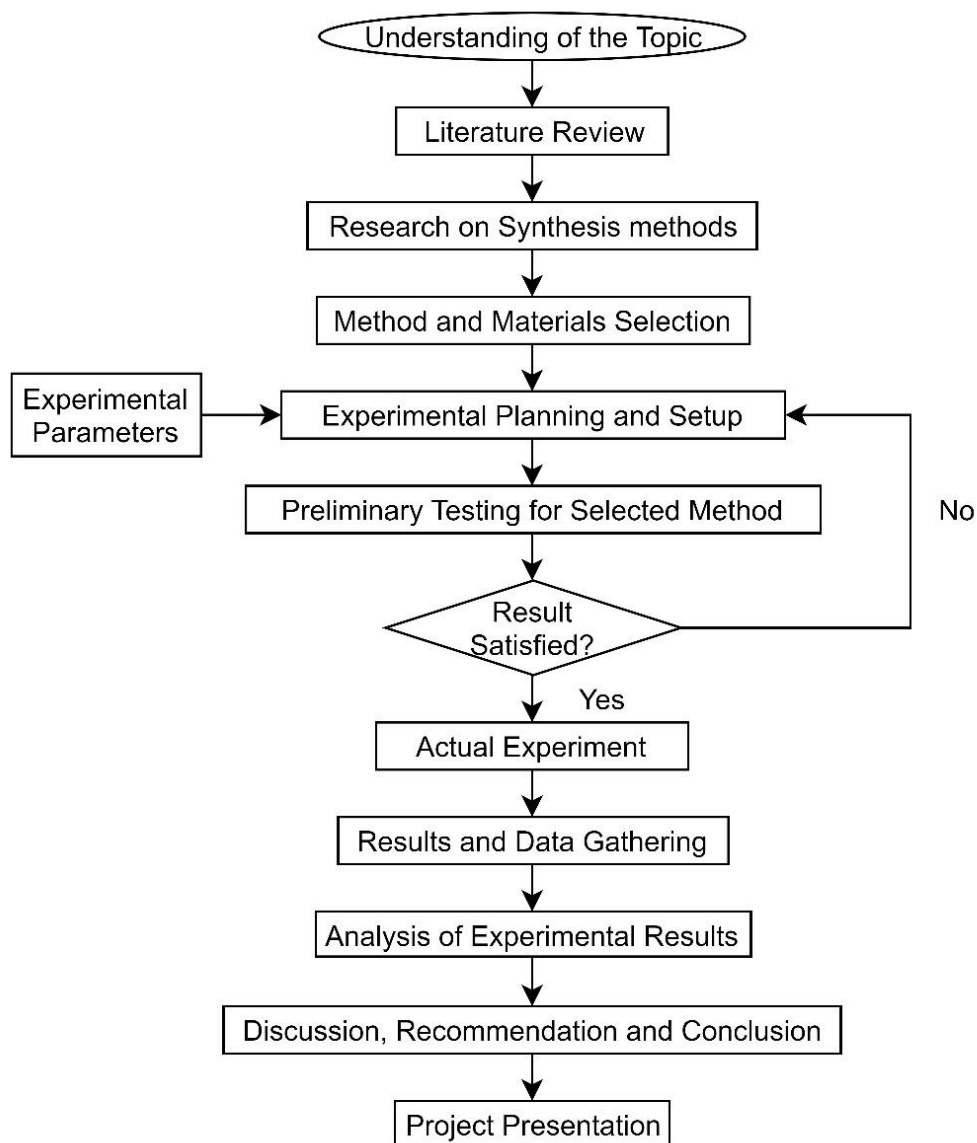


Figure 3.3: Project Flowchart

### 3.3 Materials

Table 3.1 shows the list of chemicals that were used for the experiment in this project. Chemicals listed in the table below was used to synthesis  $FeCl_3 - GIC$  and  $FeCl_3 - FLG$  through hydrothermal intercalation and microwave exfoliation method. Besides, chemicals in Table 3.1 were also used to fabricate normal capacitor,  $FeCl_3 - GIC$  supercapacitor and  $FeCl_3 - FLG$  supercapacitor.

Table 3.1: List of Chemicals

Chemicals	Specification
Activated Carbon	Powder
Deionised Water	N/A
Ethanol	99 % Purity
Graphite Powder	< 20 $\mu\text{m}$
Hydrogen Peroxide	32 % Purity
Iron (III) Chloride	Anhydrous
N, N-Dimethyl Formamide	99 % Purity
Ortho-Phosphoric Acid	85 % Purity
Polyurethane	N/A

### 3.4 Experiment Procedures

#### 3.4.1 Hydrothermal Intercalation

First of all, 10 g of graphite powder and 30 g of  $\text{FeCl}_3$  anhydrous was mixed with the aid of ethanol as the mixing agent in a 100 mL beaker. The mixtures were then transferred to a disposable bottle which contains grinding media to enhance the mixing and intercalation of the mixtures. The disposable bottle was placed on a rolling machine for 3 hours. Figure 3.4 shows the rolling machine that is rotating the disposable bottle, the duct tape on the bottle was used to increase the friction between the disposable bottle and the roller of the rolling machine as the surface of the disposable bottle and the roller are quite smooth.

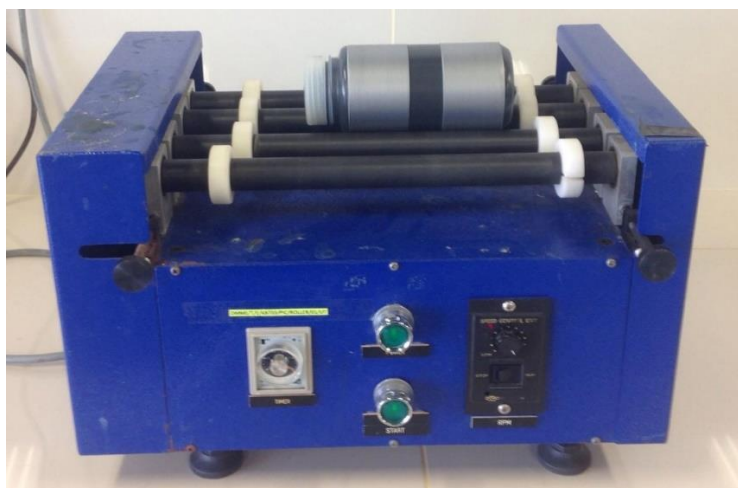


Figure 3.4: Rotating Mixtures in Disposable Bottle

The “landslide” situation will happen in the disposable bottle when the mixtures were turned by the rolling machine. As the rolling machine is rotating, the grinding media will drop to the bottom of the bottle from near the top due to gravitational force. The impact of the grinding media will reduce the size of the mixtures as it drops, smaller dimension of mixtures will increase the ability of  $FeCl_3$  molecules to intercalate between the layered structures of graphite. After the mixtures have been rotated, the grinding media was separated from the mixtures by using a flour separator. The residue mixtures that stick on the grinding media was washed and rinsed with ethanol. Figure 3.5 shows the separation of grinding media from the mixtures.



Figure 3.5: Separation of Mixtures and Grinding Media

The separated mixtures were placed into a Memmert Oven and dried for 24 hours at a temperature of 80 °C. Next, the dried sample was taken out after it was cooled down to a temperature around 45 °C to avoid thermal shock. Figure 3.6 shows the mixture that was dried for 24 hours. From the figure below, it can be observed that the mixtures were not completely dried off, there was still some moisture remained in the mixtures.



Figure 3.6: Dried Mixtures

Figure 3.7 shows the mixtures that were separated from the bowl as soon as it was removed from the oven. It can be observed that the mixtures became moist when it exposed to the atmosphere, the mixtures will absorb the water vapour that contains in the atmosphere and clumped together.



Figure 3.7: Clumped Mixtures

The mixtures were then quickly transferred into a 50 mL stainless steel autoclave and heated for 12 hours at a temperature of 180 °C. Figure 3.8 shows the stainless steel autoclave that was placed in an oven for heating purpose. The white colour Teflon vessel was used to keep the mixtures in the stainless steel autoclave.



Figure 3.8: 50 mL Stainless Steel Autoclave

Figure 3.9 shows the heated mixtures placed into the Teflon vessel. It can be observed that the mixtures were completely dried and will become powder once it was touched or compressed.



Figure 3.9: Heated Mixtures in Teflon Vessel

The heated mixtures were then rinsed and washed with deionised water after it was cooled down to room temperature to obtain  $FeCl_3 - GIC$ . Figure 3.10 shows the mixtures that was undergoing a filtration process. The main purpose of filtering the mixtures were to reduce the pH value of the mixtures as  $FeCl_3$  is acidic in nature.



Figure 3.10: Filtration of Mixtures

After the filtration process,  $FeCl_3 - GIC$  was mixed with 40 mL of N, N-Dimethyl Formamide as shown in Figure 3.11 and ultrasonicated for 3 hours to obtain  $FeCl_3 - FLG$ .



Figure 3.11:  $FeCl_3 - GIC$  Mixed with N, N-Dimethyl Formamide

Figure 3.12 shows the mixture that was immersed in an ultrasonication bath. After the ultrasonication process,  $FeCl_3 - FLG$  in solution form was dried in a conventional oven for 24 hours to obtain  $FeCl_3 - FLG$  in powder form. Figure 3.13 shows the  $FeCl_3 - FLG$  that was completely dried off.



Figure 3.12: Ultrasonication of Mixtures



Figure 3.13:  $FeCl_3$  – FLG

### 3.4.2 Microwave Exfoliation

Mixture for microwave exfoliation was prepared by mixing 10 g of graphite with 30 g of  $FeCl_3$ . Figure 3.14 shows the mixtures of graphite and  $FeCl_3$  that were mixed in a 100 mL beaker.



Figure 3.14: Mixtures of Graphite and  $FeCl_3$

The mixtures were then placed into a conventional microwave for 2 minutes. Intercalation and exfoliation process will take place at the same time during microwave irradiation. After microwave irradiation, 2 g of the mixture will be added into 250 mL of hydrogen peroxide (32 %) for further exfoliation. After 2 hours of exfoliation,  $FeCl_3 - GIC$  will be obtained.

Next, 40 mL of N, N-Dimethyl Formamide was added into  $FeCl_3 - GIC$  as a solvent to assist in exfoliation of  $FeCl_3 - GIC$ . The mixtures of N, N-Dimethyl Formamide and  $FeCl_3 - GIC$  was then ultrasonicated for 3 hours to obtain  $FeCl_3 - FLG$ .

### 3.4.3 Fabrication of Supercapacitor

Two pieces of aluminium plate with a dimension of 9 cm x 6 cm and a thickness of 0.2 cm act as a current collector for the capacitor had been drilled a hole with a diameter of 0.3 cm at the corner of each aluminium plate. A side of each aluminium plate was grinded using a piece of sandpaper to ensure the surface are rough for later use. A rivet was then used to secure a copper wire at the hole that was drilled at the corner of each aluminium plate. Figure 3.15 shows the aluminium plates that were connected to a copper wire.

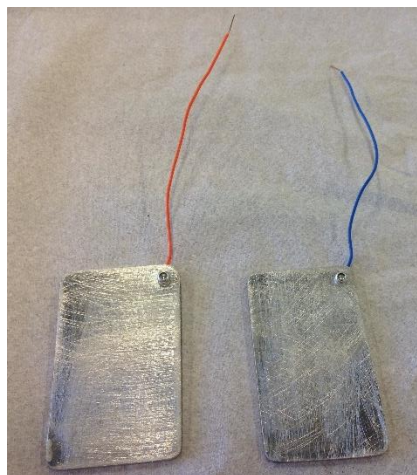


Figure 3.15: Aluminium Plates Connected to a Copper Wire

A normal capacitor was constructed by applying a thin layer of polyurethane on the rough surface of the aluminium plates. As for supercapacitor, 2 g of  $FeCl_3 - GIC$  or  $FeCl_3 - FLG$  were mixed with 5 mL of polyurethane, it was then apply on the surface of the aluminium plates. Activated carbon was immediately sprinkle on the aluminium plates of capacitor and supercapacitor and allowed it to dry off for 1 day.  $FeCl_3 - GIC$  and  $FeCl_3 - FLG$  that were used to fabricate supercapacitor was synthesised by hydrothermal intercalation method, due to the reason that the exfoliation process of microwave exfoliation required large amount of hydrogen peroxide,  $FeCl_3 - FLG$  that was synthesised by microwave exfoliation method was not enough to fabricate a supercapacitor. Therefore, the supercapacitor can only be fabricated using  $FeCl_3 - GIC$  and  $FeCl_3 - FLG$  that were synthesised through hydrothermal intercalation method. Figure 3.16 shows the aluminium plates that were painted a thin layer of  $FeCl_3 - FLG$  on it.



Figure 3.16: Aluminium Plates with a Layer of  $FeCl_3 - FLG$

Next, the aluminium plate that was applied by polyurethane,  $FeCl_3 - GIC$  or  $FeCl_3 - FLG$  act as the anode or cathode material for the capacitor or supercapacitor. A piece of cloth that was soaked into ortho-phosphoric acid (85 %) was sandwiched between the anode and cathode material of the capacitor and supercapacitor. The function of the soaked cloth was to prevent the anode material from contacting with the cathode material and cause a short circuit. Whereas, the function of ortho-phosphoric acid was to act as an electrolyte to allow the charge to pass through the cloth.

The capacitor and supercapacitor were then sealed by using a plastic bag to prevent the acid electrolyte to escape when evaporated. Figure 3.17 shows the  $FeCl_3 - FLG$  supercapacitor that was sealed in a plastic bag.



Figure 3.17: Sealed  $FeCl_3 - FLG$  Supercapacitor

Since the output voltage of a capacitor and supercapacitor is very less, therefore, normal discharge method cannot apply. The capacitor and supercapacitor in this project are to be discharged naturally, the voltage of the capacitor and supercapacitor while discharging is measured by a multimeter in parallel to the capacitor. Figure 3.18 shows the setup of measuring the voltage of a discharging supercapacitor.

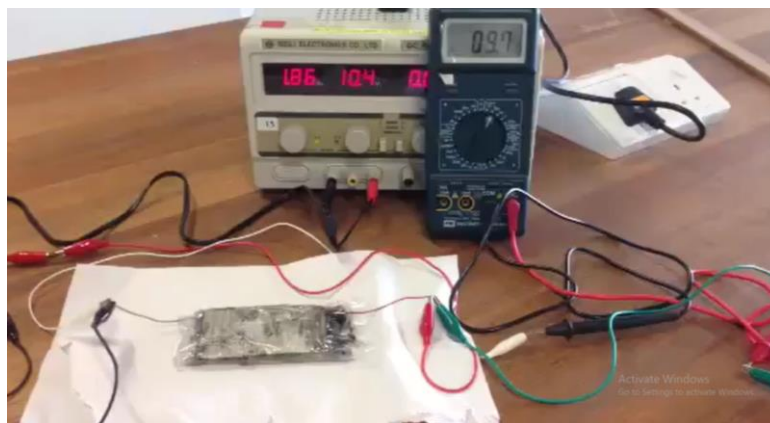


Figure 3.18: Setup of Discharging  $FeCl_3 - FLG$  Supercapacitor

## 3.5 Characterisations

### 3.5.1 Scanning Electron Microscope

Scanning Electron Microscope (SEM) was used in this project to determine the morphology of graphite,  $FeCl_3 - GIC$  and  $FeCl_3 - FLG$ , it was also used to determine the number of layer of  $FeCl_3 - FLG$  from the edges of the samples. The samples powder were dropped lightly on the aluminium holder that had the double-sided tape. It was then blown by a manual rubber bulb air pump to remove the excess samples on the surface in order to ensure the thickness of the samples will not exceed the standard thickness. The samples were not coated with anything because it conducts electricity in nature.

The image of samples was taken at the magnification in the range of 10 000x to 30 000x with an accelerating voltage of 15 kV by using the SEM equipment (Hitachi S-3 400N) in UTAR KB 732 as shown in Figure 3.19.



Figure 3.19: UTAR SEM

### 3.5.2 Field-Emission Scanning Electron Microscope

Field-Emission Scanning Electron Microscope (FESEM) was used to conduct a nanoscale analysis on  $FeCl_3 - FLG$ . In order to ensure that it is few layers rather than multi-layer structure, the magnification was increased to the range of 30 000x to 70 000x with an accelerating voltage of 2 kV.

The preparation method and procedure for FESEM sample was the same as the preparation of samples for SEM. The FESEM equipment (JEOL JSM 7800F PRIME) is located at Universiti Teknologi Malaysia (UTM) Microscopy Laboratory Level 01.29.01 as shown in Figure 3.20.



Figure 3.20: UTM FESEM

### 3.5.3 Energy Dispersive X-Ray Spectroscopy

Energy Dispersive X-Ray Spectroscopy (EDX) was utilised in this project to analyse the elements in the  $FeCl_3 - GIC$  and  $FeCl_3 - FLG$  samples. EDX is a technology that use to determine the elements and characterise the chemical of a sample. It normally uses together with SEM or FESEM. As the sample is bombarded by an electron beam, EDX analysed the X-rays that was emitted from the sample and characterize the elemental composition of the targeted volume (Goldstein, et al., 2017).

### 3.5.4 X-Ray Diffraction

Shidmazu XRD-6 000 as shown in Figure 3.21 was used in this project to perform X-Ray Diffraction (XRD) analysis.



Figure 3.21: UTAR XRD

Graphite,  $FeCl_3 - GIC$  and  $FeCl_3 - FLG$  powder was filled into the XRD holder to perform XRD analysis. The holder is compressed by using a thick square piece of glass to ensure that it is dense and flat. Figure 3.22 shows the prepared  $FeCl_3 - FLG$  XRD sample.

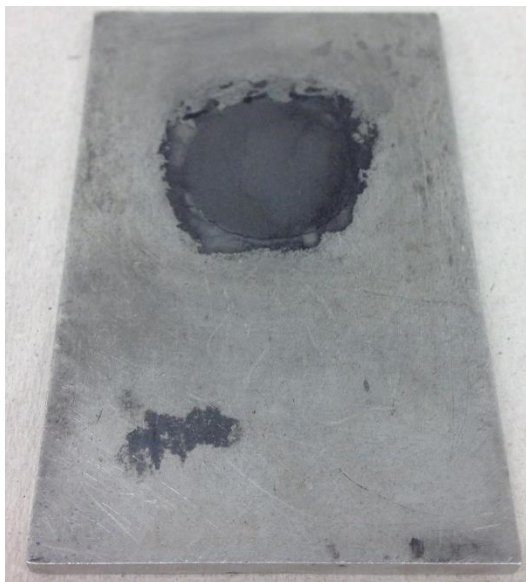


Figure 3.22:  $FeCl_3$  – FLG XRD Sample

The samples were then analysed in the scanning range of  $10^\circ$  to  $80^\circ$ , the scanning range is to be represented by  $2\theta$ . The machine used nickel filtered copper  $K\alpha$  radiation which has a wavelength of 0.154 nm at a scanning speed of 2 degree/min to scan the samples. Equation 3.1 was used to calculate the interlayer spacing, which is based on Bragg's equation:

$$d = \frac{\lambda}{2 \sin \theta} \quad (3.1)$$

Where:

$d$  = spacing between the layers of atom

$\lambda$  = wavelength of the X-rays (0.154 nm)

$\theta$  = angle between the crystal surface and incident rays

### 3.5.5 Fourier Transform Infrared Spectroscopy

Nicolet IS10 was used to conduct Fourier Transform Infrared Spectroscopy (FTIR) analysis in this project to identify the types of functional groups and chemical bonds contain in the graphite,  $FeCl_3$  – GIC and  $FeCl_3$  – FLG powder. The analysis was carried in the wavelength range of  $4\,000\text{ cm}^{-1}$  and  $500\text{ cm}^{-1}$ . The background spectrum was captured before the samples were scanned. Figure 3.23 shows the FTIR equipment that is located in UTAR KB 511.



Figure 3.23: UTAR FTIR

## CHAPTER 4

### RESULTS AND DISCUSSIONS

#### 4.1 Comparison of Different Synthesis Methods

In this project, there are two methods that were performed to synthesis  $FeCl_3 - FLG$ . The first method was hydrothermal intercalation where intercalation of  $FeCl_3$  into the layered structure of graphite occurred during the heating process. When the mixtures of graphite and  $FeCl_3$  were heated in the oven, the process of intercalation of  $FeCl_3$  into the layered structure of graphite will produced  $FeCl_3 - GIC$ . It was then ultrasonicated for 3 hours to obtain  $FeCl_3 - FLG$ .

The second method was the microwave exfoliation method. It was a method that used microwave irradiation to exfoliate the layered structure of graphite and intercalate  $FeCl_3$  between the layers of graphite. The mixture was then added into hydrogen peroxide to exfoliate into  $FeCl_3 - GIC$ . The obtained  $FeCl_3 - GIC$  was then ultrasonicated for 3 hours to get  $FeCl_3 - FLG$ .

By comparing the hydrothermal intercalation and microwave exfoliation method, the hydrothermal intercalation method was a better method to synthesis  $FeCl_3 - FLG$ . Exfoliation of the mixture into  $FeCl_3 - GIC$  using hydrogen peroxide for microwave exfoliation method required a large amount of hydrogen peroxide. 2 g  $FeCl_3 - GIC$  required 250 mL of hydrogen peroxide for exfoliation. Microwave exfoliation method is suitable for laboratory research that require a small amount of sample, whereas hydrothermal intercalation is more suitable to be synthesis in large quantity for industries manufacturing use.

#### 4.2 Characterisations

##### 4.2.1 Scanning Electron Microscope

Morphology of graphite was determined by using SEM in UTAR. Figure 4.1 and Figure 4.2 shows the edges of graphite flakes that did not undergo any processes. Figure 4.1 shows that at the magnification of 11 000x, it can be observed that the graphite flake are a layered structure that is stacked together in a parallel manner. The number of layers of graphite is difficult to be determined as it is stacked compactly.

However, it can be confirmed as graphite because it is a bulk combination of graphene layers and the number of layers is obviously more than 10 layers (Goh and Pumera, 2010).

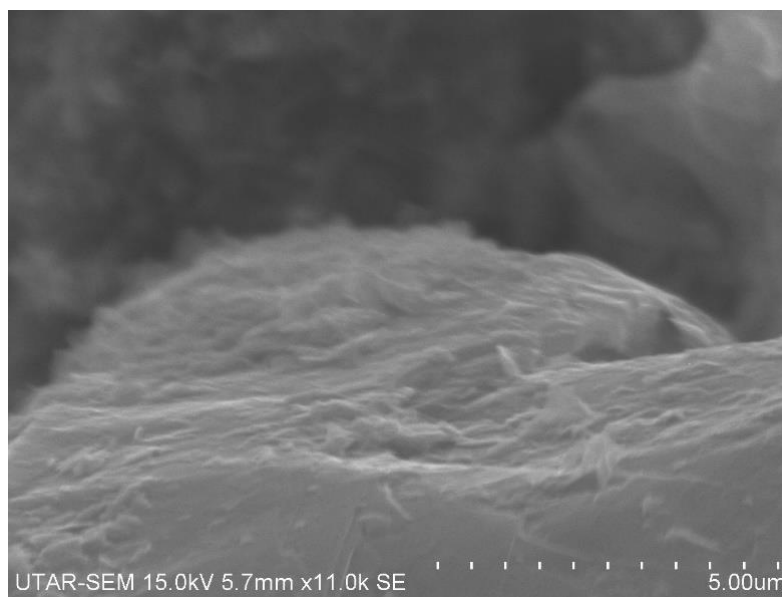


Figure 4.1: Graphite SEM Image at the Magnification of 11 000x

Whereas Figure 4.2 shows that at the magnification of 25 000x, it can be observed that there are no foreign substances or contamination on or around the graphite flake. It is formed purely by the stacking of graphene sheets without any combination or mixture of any noticeable atoms and molecules.

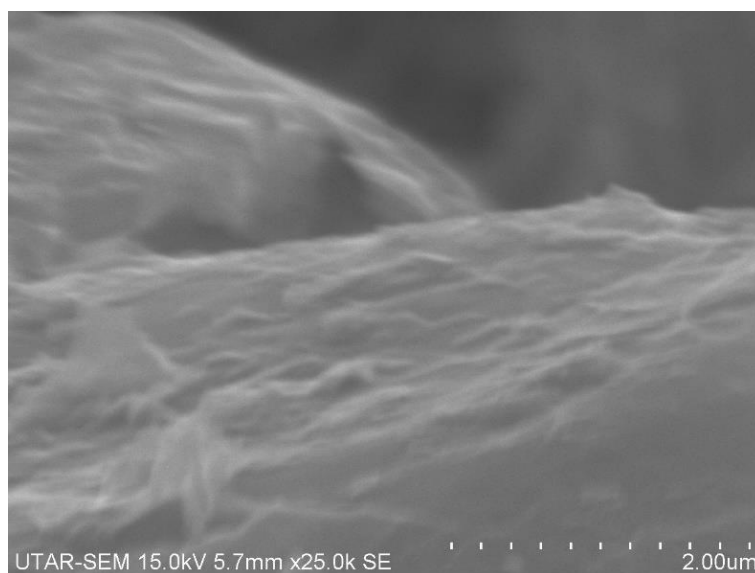


Figure 4.2: Graphite SEM Image at the Magnification of 25 000x

After graphite and  $FeCl_3$  was mixed with ethanol and rotate for 3 hours, it was heated at 80 °C for 24 hours in a conventional oven. After 24 hours of heating, the mixtures was transferred rapidly into an autoclave to avoid excessive exposure to air. Due to the reason that the mixtures contain  $FeCl_3$ , it tend to attract water or water vapour around the surrounding and become moist eventually (Frank, et al., 2007). Therefore, it is best to minimise the exposure of mixtures to the surrounding and moist surface. After transferring the mixtures into an autoclave, it was then heated at 180 °C for 12 hours.  $FeCl_3 - GIC$  will be formed after the heating process. Heating is a significant process in this experiment as the intercalation process took place when the mixture was heated (Wei, et al., 2008).

The synthesised  $FeCl_3 - GIC$  was then observed using SEM at the magnification of 9 500x, 14 000x and 17 000x. Figure 4.3 shows the SEM image of  $FeCl_3 - GIC$  at the magnification of 9 500x. It can be observed that  $FeCl_3$  was intercalated between the layered structures of graphite. After  $FeCl_3$  intercalated between the layers of graphite, the distance between the layers had increase and hence easier to be separated as compared to graphite.

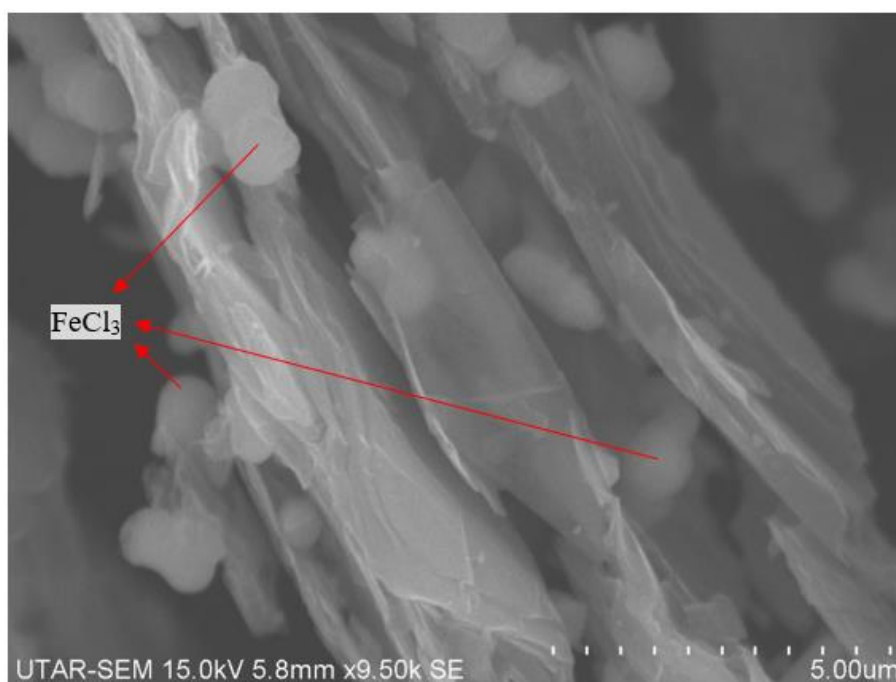


Figure 4.3:  $FeCl_3 - GIC$  SEM Image at the Magnification of 9 500x

Figure 4.4 and Figure 4.5 show that the total layers of  $FeCl_3 - GIC$  had reduced significantly as compared to graphite flakes. There are also some  $FeCl_3$  can be observed on the surface of  $FeCl_3 - GIC$ .

When the magnification increased to 14 000x and 17 000x as shown in Figure 4.4 and Figure 4.5, respectively, cracks can be observed on the surface of the layers, it may result from the heating and intercalation process.

It is hypothesised that during the heating process, the molecules of graphite absorb the heat energy, and hence molecules of graphite vibrate faster. The vibration of molecules increases the space between the molecules, vibration and spacing of the molecules results in the expansion of graphite.

Intercalation process occurred as the mixtures were heated. The intercalant,  $FeCl_3$  will tend to squeeze into the layers of graphite. The squeezing of intercalant may exert forces to the surface of graphite. When both heating and intercalation process occurred at the same time, the forces of heating and intercalation process will results in cracking on the surface.

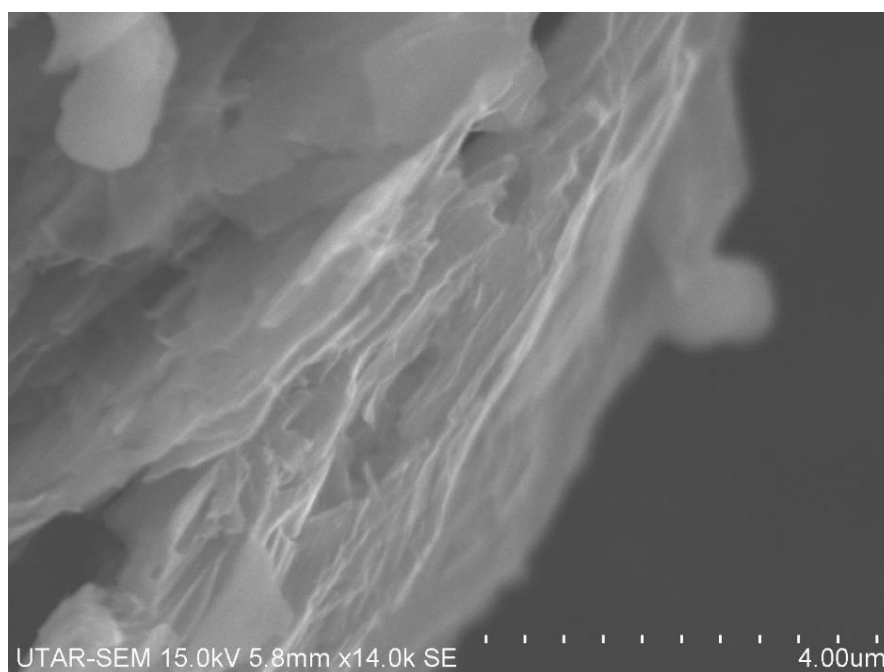


Figure 4.4:  $FeCl_3 - GIC$  SEM Image at the Magnification of 14 000x

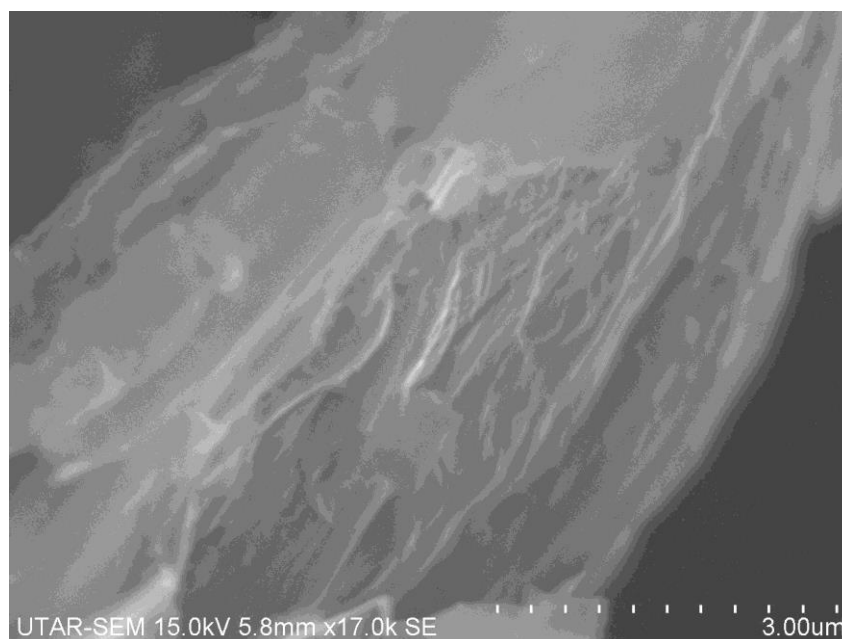


Figure 4.5:  $FeCl_3$  – GIC SEM Image at the Magnification of 17 000x

$FeCl_3$  – GIC was then mixed with N, N-Dimethyl Formamide for ultrasonication process. The most effective way for a successful exfoliation is to overcome the weak van der Waals forces between the adjacent planes. N, N-Dimethyl Formamide was chosen because it has a surface tension value of  $\gamma = 37.1 \text{ mJm}^{-2}$ , which is proven to be the most suitable solvent for dispersing graphite flakes (Ciesielski and Samorì, 2014).

The ultrasonication process was conducted for 3 hours to obtain  $FeCl_3$  – FLG. Figure 4.6 and Figure 4.7 show the SEM images of  $FeCl_3$  – FLG at the magnification of 27 000x and 42 000x, respectively. Although there are some cracks on the surface, a layer of graphene was successfully separated out from the layered structure of graphite.



Figure 4.6: Graphene SEM Image at the Magnification of 27 000x

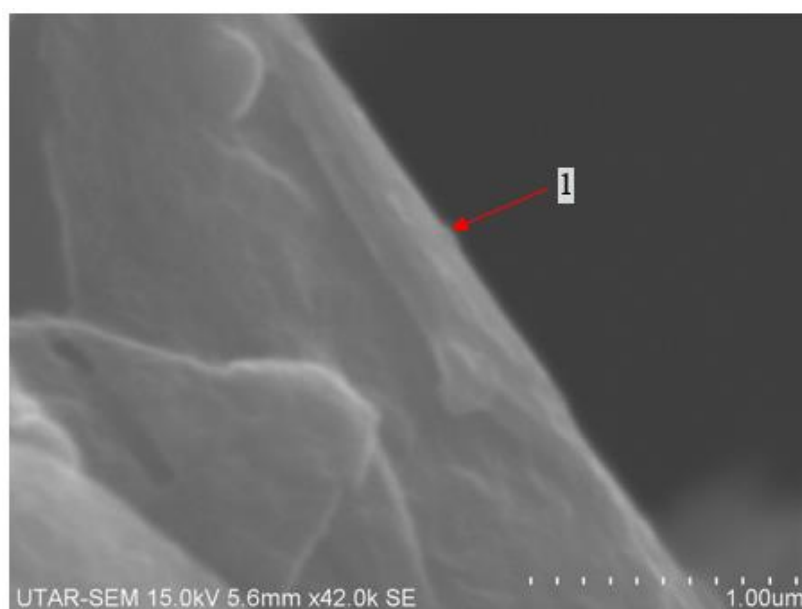


Figure 4.7: Graphene SEM Image at the Magnification of 42 000x

Figure 4.8 and Figure 4.9 show the SEM images of  $FeCl_3 - FLG$  at the magnification of 16 000x and 23 000x, respectively. From the figures below, it can be observed that the layers of graphene are 3 to 4 layers, which can be categorised as FLG. Compared to the graphene sheet in Figure 4.6 and Figure 4.7, the number of layers of graphene in Figure 4.8 and Figure 4.9 are greater. It is hypothesised that the time of ultrasonication process will affect the quality and number of layers of graphene.

Although all the GIC are synthesised from the same graphite powder, however, some GIC might have more layers compared to other GIC. Therefore, some GIC might require more energy to exfoliate due to the additional layers to be separated.

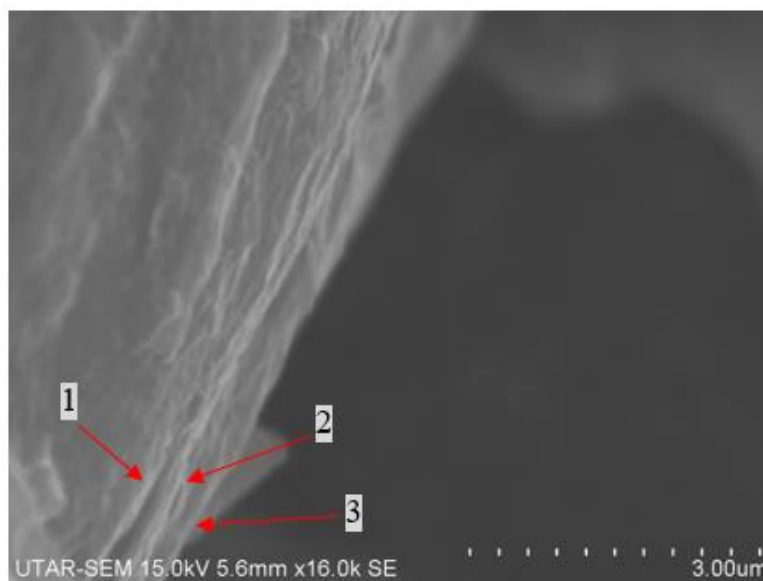


Figure 4.8:  $FeCl_3$  – FLG SEM Image at the Magnification of 16 000x

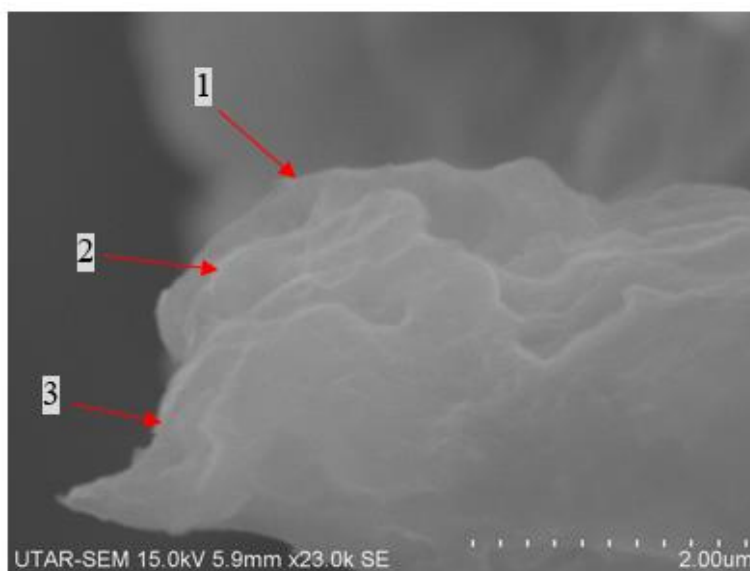


Figure 4.9:  $FeCl_3$  – FLG SEM Image at the Magnification of 23 000x

Figure 4.10 and Figure 4.11 show the SEM images of  $FeCl_3$  – FLG at the magnification of 50 000x and 32 000x, respectively. From the figures below, it can be observed that there are some foreign substance on the surface and between the layers

of graphene sheets. It is hypothesised that the foreign substances are the remaining  $FeCl_3$  that had undergoes the ultrasonication process. Before the ultrasonication process,  $FeCl_3$  were lumped together and appeared to be bigger in size and spherical in shape. However, after  $FeCl_3$  had undergone ultrasonication process, it disintegrate and break down into a smaller size. There are a portion of  $FeCl_3$  remained in the samples, while other were removed during the filtering process.

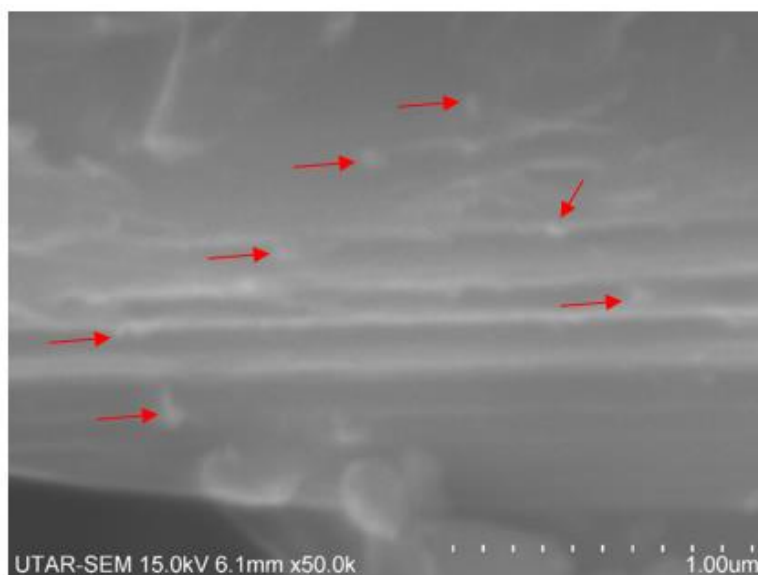


Figure 4.10:  $FeCl_3$  – FLG SEM Image at the Magnification of 50 000x

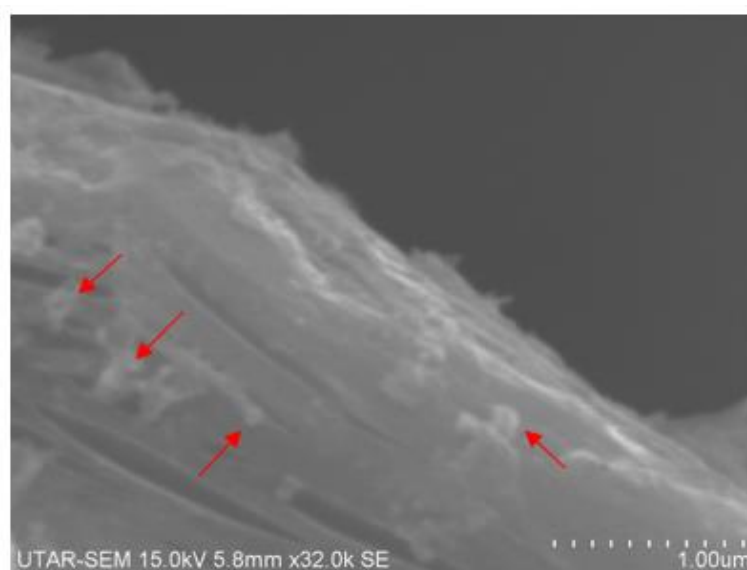


Figure 4.11:  $FeCl_3$  – FLG SEM Image at the Magnification of 32 000x

### 4.2.2 Field-Emission Scanning Electron Microscope

FESEM in UTM was used to further investigate the topography and morphology of the synthesised  $FeCl_3 - FLG$ . Due to the reason that FESEM in UTAR Kampar was under maintenance, the observation of  $FeCl_3 - FLG$  can only be done in other research centre or university such as UTM. The reason that FESEM was used is to guarantee the quality of synthesised  $FeCl_3 - FLG$  and to have a clearer image of the assured  $FeCl_3 - FLG$ .

Figure 4.12 shows the FESEM image of  $FeCl_3 - FLG$  at the magnification of 70 000x. From the figure below, it can be clearly observed that there are only a single layer of graphene shown in the image, therefore, it can be ensured that there are SLG presented in the sample.

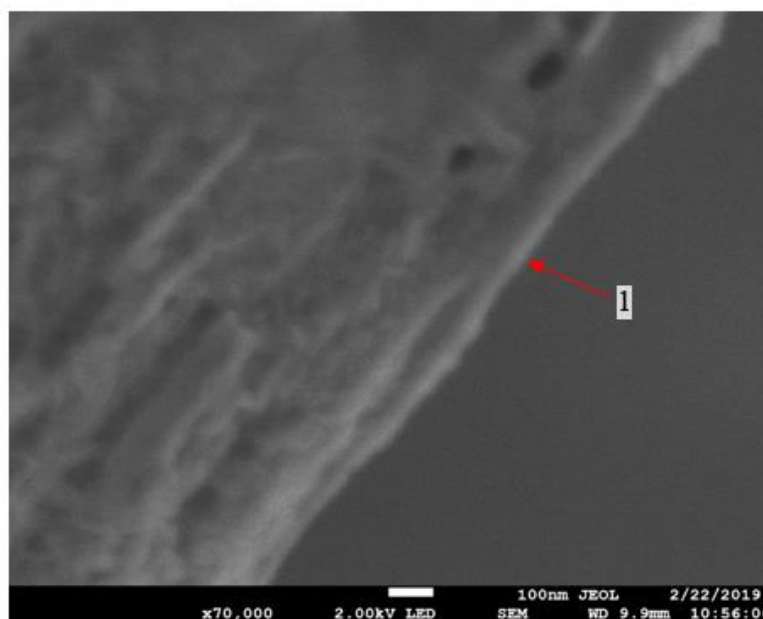


Figure 4.12:  $FeCl_3 - FLG$  FESEM Image at the Magnification of 70 000x

Moreover, Figure 4.13 shows the FESEM image of  $FeCl_3 - FLG$  at the magnification of 40 000x. From the figure below, it can be observed that there are 2 layers of graphene sheet that stacked together and form a bilayer graphene.

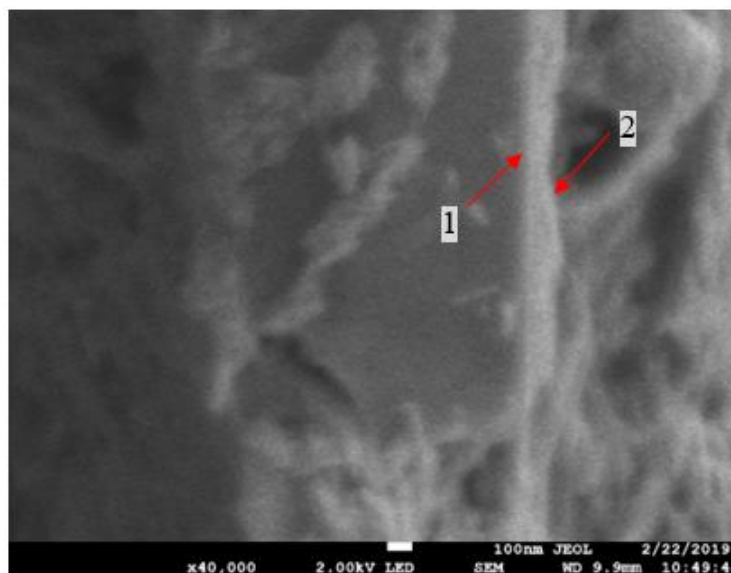


Figure 4.13:  $FeCl_3$  – FLG FESEM Image at the Magnification of 40 000x

Figure 4.14 shows the FESEM image of  $FeCl_3$ -FLG at the magnification of 55 000x. From the figure below, it can be observed that this  $FeCl_3$  – FLG was formed by the stacking of 3 layers of graphene sheet.

Besides, from Figure 4.14, it can be observed that there are some foreign matters presented on some of the surfaces of the graphene sheets. It is hypothesised that the foreign matter is N, N-Dimethyl Formamide, as it was dried off during the drying process, the remains might remain or stick on some of the surfaces of the graphene sheets

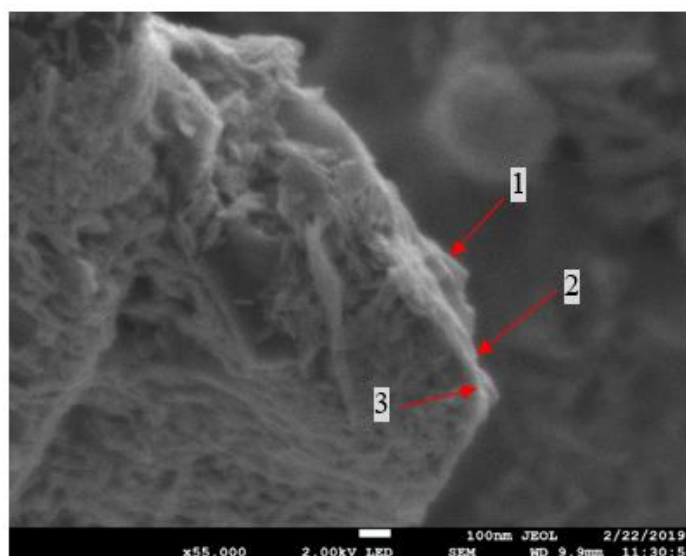


Figure 4.14:  $FeCl_3$  – FLG FESEM Image at the Magnification of 55 000x

### 4.2.3 Energy Dispersive X-Ray Spectroscopy

Figure 4.15 shows the SEM images of  $FeCl_3 - GIC$  and  $FeCl_3 - FLG$ , respectively. The SEM images represent the area that was focused by EDX for elemental analysis.

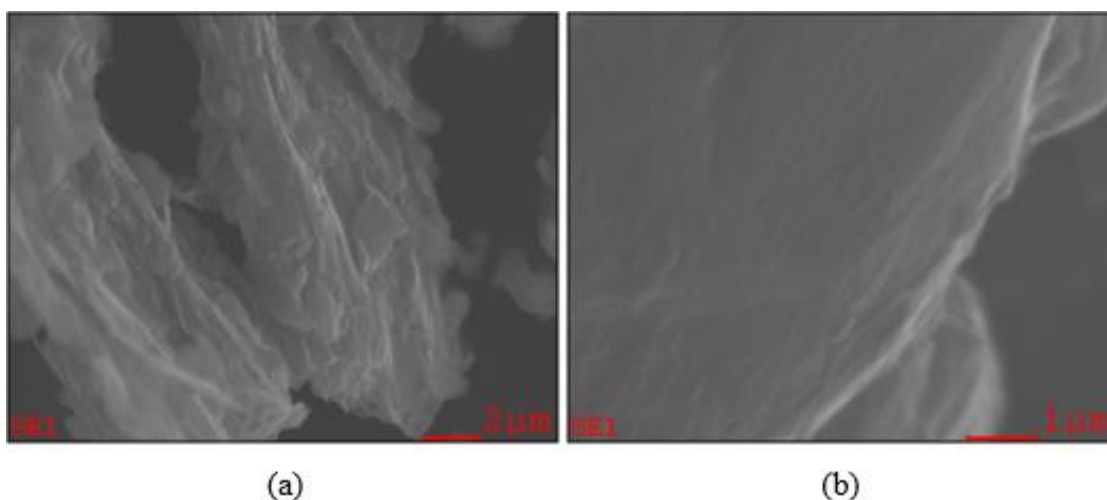


Figure 4.15: SEM Image of (a)  $FeCl_3 - GIC$  and (b)  $FeCl_3 - FLG$  for EDX

The elemental analysis is categorised into atomic percentage (At %) weight percentage (Wt %). Table 4.1 shows Wt for  $FeCl_3 - GIC$  and  $FeCl_3 - FLG$ .

Table 4.1 summarised Wt % of  $FeCl_3 - GIC$  and  $FeCl_3 - FLG$  for carbon, oxygen, chlorine and ferric, respectively. The Wt % of  $FeCl_3$ -GIC for carbon, oxygen, chlorine and ferric are 61 %, 11.36 %, 7.25 % and 20.39 %, respectively. Whereas, the Wt % of  $FeCl_3$ -FLG are 36.37 %, 3.69 %, 32.76 % and 27.18 %, respectively.

From the information provided by the elemental analysis of EDX, it can be summarised that other than  $FeCl_3$  that had been intercalated into the layered structure of graphite, which is formed by carbon atoms, there are also a small amount of oxygen contained in the sample too. It is hypothesised that the small amount of oxygen content may be due to the oxidation of  $FeCl_3$ .

By comparing the Wt % between  $FeCl_3 - GIC$  and  $FeCl_3 - FLG$ , it can be analysed that the percentage of carbon atom in  $FeCl_3 - GIC$  is higher. It is hypothesised that in a selected area, the total number of carbon atoms contained in  $FeCl_3 - GIC$  is higher compared to  $FeCl_3 - FLG$ . This is due to the reason that the distance between the layers of  $FeCl_3 - GIC$  is smaller compared to  $FeCl_3 - FLG$ ,

thus,  $FeCl_3 - GIC$  will contain more carbon atoms in a fixed space compared to  $FeCl_3 - FLG$ .

Table 4.1: EDX Elemental Analysis of  $FeCl_3 - GIC$  and  $FeCl_3 - FLG$  in Wt%

Element	Composition (Wt %)	
	$FeCl_3 - GIC$	$FeCl_3 - FLG$
Carbon	61.00	36.37
Oxygen	11.36	3.69
Chlorine	7.25	32.76
Ferric	20.39	27.18
Total	100.00	100.00

#### 4.2.4 X-Ray Diffraction

Figure 4.16 shows the XRD Diffractogram of graphite powder and Joint Committee on Powder Diffraction Standards (JCPDS) card of carbon. The graphite powder that provided by UTAR was analysed by XRD and matched with JCPDS card of carbon using HighScore Plus software.

From Figure 4.16, it can be observed that there are 2 obvious peaks. The first peak was located at  $2\theta = 26.58^\circ$ , where the second peak was at  $2\theta = 54.66^\circ$ . The first peak at  $2\theta = 26.58^\circ$  corresponds to the spacing between the layered structure of graphite, which is around 0.335 nm. After the graphite powder was analysed by using XRD, it was matched with the database of HighScore Plus to search for similar elements that exist in the sample.

The matching result shows that the sample contained carbon, where the peaks of carbon matched with the peaks of graphite powder at  $2\theta = 26.38^\circ$  and  $2\theta = 54.54^\circ$ . From the results of XRD, it can be concluded that the graphite powder contained only carbon element because there was no other element that matched with the XRD Diffractogram of graphite.

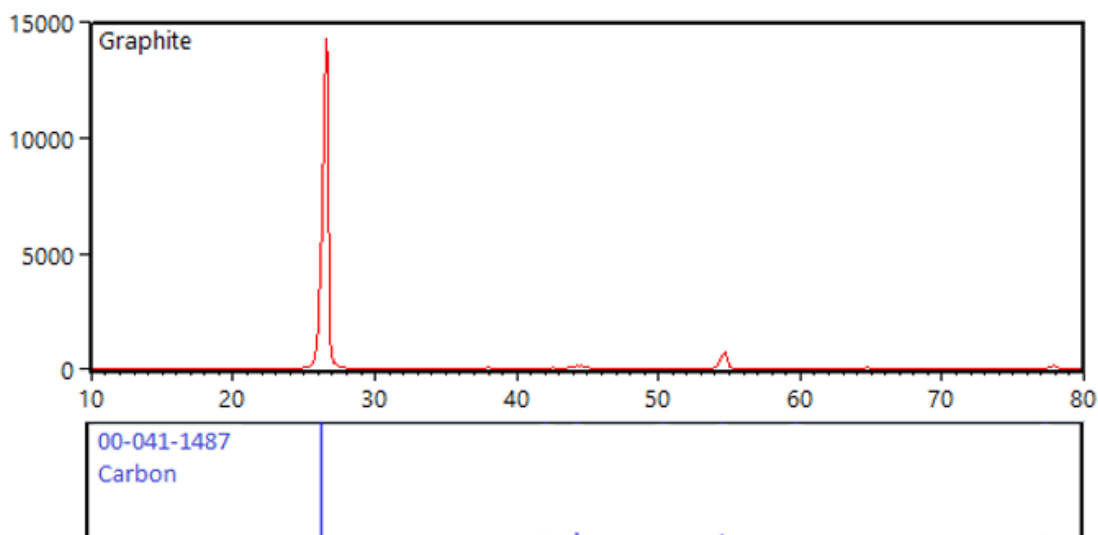


Figure 4.16: XRD Diffractogram of Graphite and JCPDS Card of Carbon

Figure 4.17 shows the XRD Diffractogram of  $FeCl_3 - GIC$  and JCPDS cards of carbon and iron oxide. From Figure 4.16 and Figure 4.17, it can be observed that the XRD Diffractogram of graphite and  $FeCl_3 - GIC$  are almost similar. The 2 obvious peaks of  $FeCl_3 - GIC$  was located at  $2\theta = 26.78^\circ$  and  $2\theta = 54.90^\circ$ .

The XRD Diffractogram of  $FeCl_3 - GIC$  was analysed by HighScore Plus software to determine the elements that matched with the sample. The result shows that there are 2 elements that matched with it, which were carbon and iron oxide. Among the peaks of carbon, the peaks that matched with peaks of  $FeCl_3 - GIC$  were the same peaks that matched with graphite, which were at  $2\theta = 26.38^\circ$  and  $2\theta = 54.54^\circ$ .

Furthermore, there were also peaks of iron oxide that matched with  $FeCl_3 - GIC$  between the range of  $2\theta = 27^\circ$  and  $2\theta = 38^\circ$ . The peaks of iron oxide that matched with  $FeCl_3 - GIC$  were at  $2\theta = 30.04^\circ$  and  $2\theta = 35.38^\circ$ . However, the reason that the peaks was not noticeable was due to the large intensity value of  $FeCl_3 - GIC$  that causes the peaks that matched with  $FeCl_3 - GIC$  difficult to be noticed.

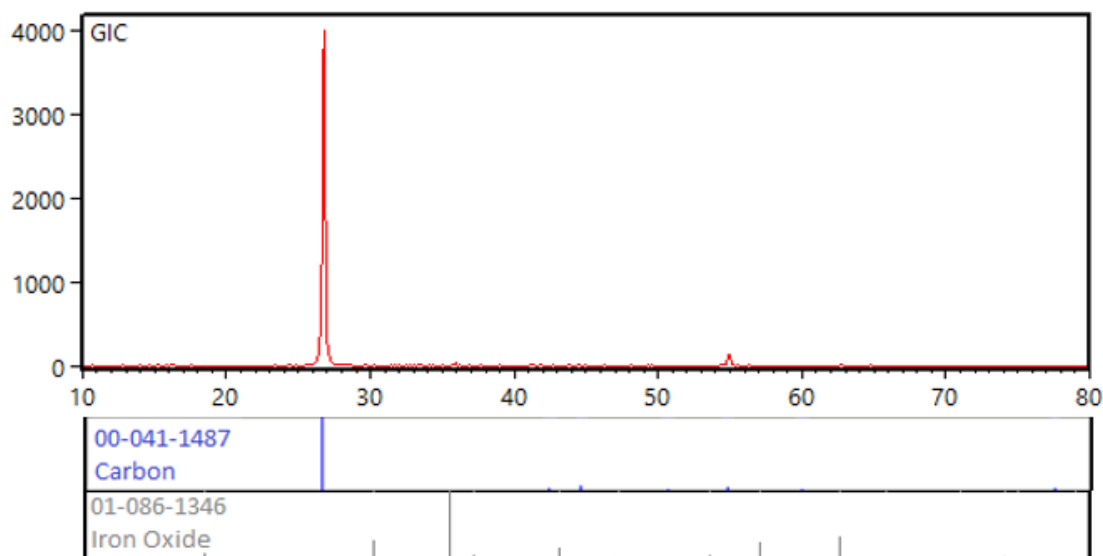


Figure 4.17: XRD Diffractogram of  $FeCl_3$  – GIC and JCPDS Cards of Carbon and Iron Oxide

Figure 4.18 shows the XRD Diffractogram of  $FeCl_3$  – FLG and JCPDS cards of carbon, chlorine and iron oxide. By comparing XRD Diffractogram of  $FeCl_3$  – FLG in Figure 4.18 with graphite in Figure 4.16 and  $FeCl_3$  – GIC in Figure 4.17, it can be observed that the maximum intensity had been reducing from graphite (14 284) to  $FeCl_3$  – GIC (3994) and finally drop to  $FeCl_3$  – FLG with the maximum intensity of 264 arbitrary unit (a.u.).

The reason that graphite has high intensity value is due to the compact layered structure of graphite. The compact layered structure of graphite have more carbon atoms compared to intercalated GIC and exfoliated FLG. Therefore, theoretically, graphite should have the highest intensity value and  $FeCl_3$  – FLG should have the lowest intensity value. From the experimental results that was obtained by XRD, it shows that graphite has the highest intensity value among the 3 of them, followed by  $FeCl_3$  – GIC and finally  $FeCl_3$  – FLG has the lowest intensity value, which correspond to the theoretical results.

From Figure 4.18, it can be observed that as the high intensity value of graphite had been reduced to lower intensity of  $FeCl_3$  – FLG, other peaks can be observed clearly. The most obvious peaks was located at  $2\theta = 13.12^\circ$ ,  $2\theta = 15.46^\circ$ ,  $2\theta = 16.92^\circ$ ,  $2\theta = 20.64^\circ$ ,  $2\theta = 26.66^\circ$ ,  $2\theta = 27.98^\circ$ ,  $2\theta = 33.92^\circ$ ,  $2\theta = 35.94^\circ$ ,  $2\theta = 36.16^\circ$  and  $2\theta = 65.66^\circ$ .

From Figure 4.18, it can be observed that the element that matched with the peaks of  $FeCl_3 - FLG$  were carbon, iron oxide and chlorine. The peak of carbon that matched with  $FeCl_3 - FLG$  peak was at  $2\theta = 26.38^\circ$ . Whereas, peaks of iron oxide that matched with  $FeCl_3 - FLG$  were at  $2\theta = 35.38^\circ$  and  $2\theta = 65.64^\circ$ . Peaks of chlorine that matched with peaks of  $FeCl_3 - FLG$  were at  $2\theta = 28.34^\circ$  and  $2\theta = 36.01^\circ$ .

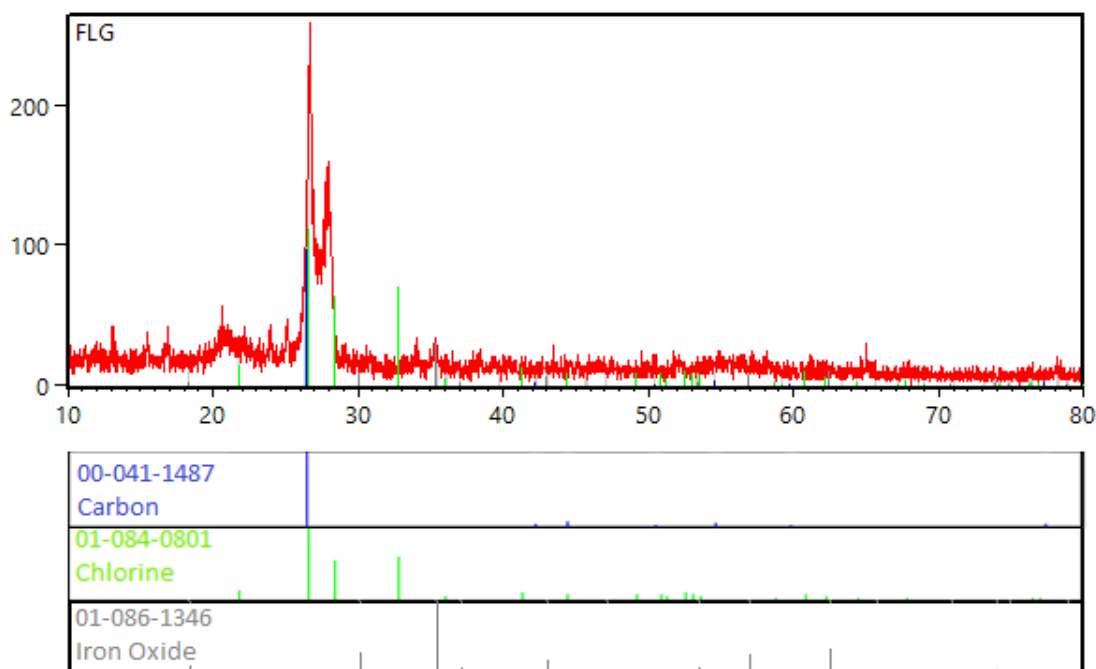


Figure 4.18: XRD Diffractogram of  $FeCl_3 - FLG$  and JCPDS Cards of Carbon, Chlorine and Iron Oxide

#### 4.2.5 Fourier Transform Infrared Spectroscopy

FTIR was carried out to determine the functional groups and chemical bonds of  $FeCl_3 - GIC$  and  $FeCl_3 - FLG$ . Besides, it also can be used to identify the formation of any GO. The scanning wavelength range for both samples were ranged from  $4000\text{ cm}^{-1}$  to  $500\text{ cm}^{-1}$ .

Figure 4.19 and Figure 4.20 show the IR spectra of  $FeCl_3 - GIC$  and  $FeCl_3 - FLG$ , respectively. From both of the figures, it can be observed that there are no functional groups formed in both samples. Therefore, it can be concluded that both  $FeCl_3 - GIC$  and  $FeCl_3 - FLG$  were not oxidise and thus, the possibility of the formation of GO can be eliminated. This can be supported by the IR spectra results of

GO that was obtained by Rattana., et al. (2012) as shown in Figure 4.21. From Figure 4.21, it can be observed that the peaks  $FeCl_3 - GIC$  and  $FeCl_3 - FLG$  are completely different with the peaks of GO. Therefore, the formation of GO can be excluded.

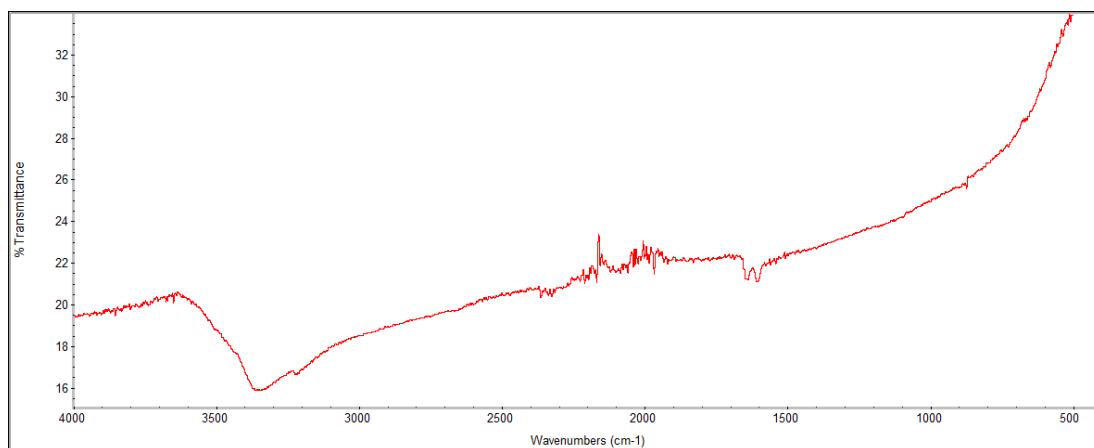


Figure 4.19:  $FeCl_3 - GIC$  IR Spectra

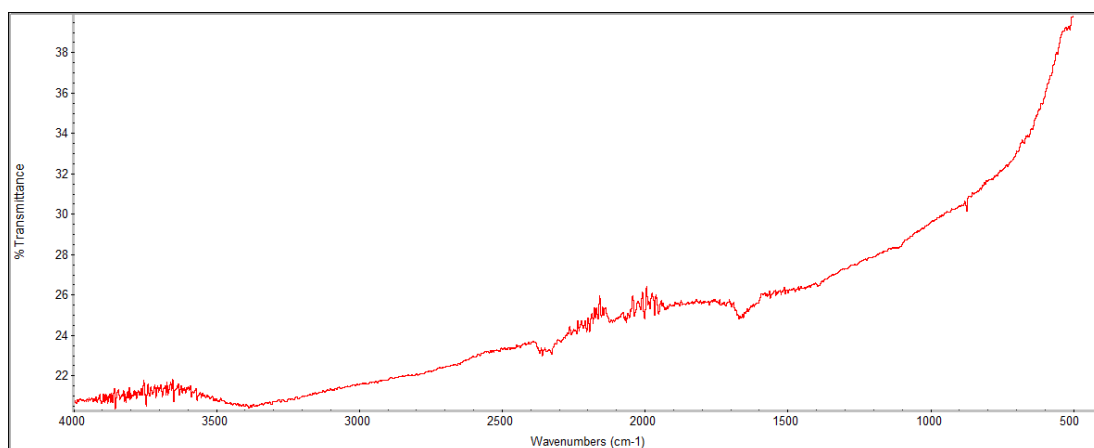


Figure 4.20:  $FeCl_3 - FLG$  IR Spectra

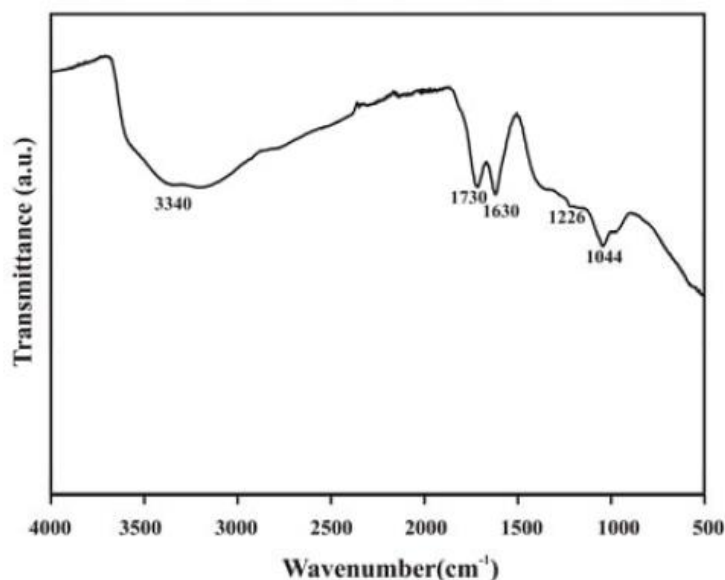


Figure 4.21: GO IR Spectra (Rattana, et al., 2012)

### 4.3 Supercapacitor

Synthesised  $FeCl_3 - GIC$  and  $FeCl_3 - FLG$  were used to fabricate supercapacitor in this project. The construction of supercapacitor using  $FeCl_3 - GIC$  and  $FeCl_3 - FLG$  has not been performed by any researcher or scientist before, as this is the first  $FeCl_3 - GIC$  and  $FeCl_3 - FLG$  supercapacitor, the performance of these supercapacitor were used to compare with a normal capacitor to investigate the improvement of using  $FeCl_3 - GIC$  and  $FeCl_3 - FLG$  to fabricate a supercapacitor.

The performance of the capacitors was determined by measuring the charging and discharging rate. In this project, the charging rate was fixed at 29 V for 10 minutes for every capacitor. Due to the low voltage output of the capacitor, the capacitor is not capable to run any motor or light-emitting diode, therefore, it was allowed to discharge naturally. The voltage and time of the discharging capacitor were recorded and measured to determine the performance of the capacitor.

Figure 4.22 shows the discharge curve of a normal symmetric capacitor that did not include any synthesised  $FeCl_3 - GIC$  and  $FeCl_3 - FLG$ . The capacitor was charged for 10 minutes at 29 V. After charging, the capacitor was allowed to discharge naturally and the discharge curve in Figure 4.22 was plotted.

From the discharge curve in Figure 4.22, it can be observed that the voltage of the capacitor drops rapidly from 375 mV to 29 mV in the first 20 seconds. It was then decreased very slowly and maintained at around 5 mV.

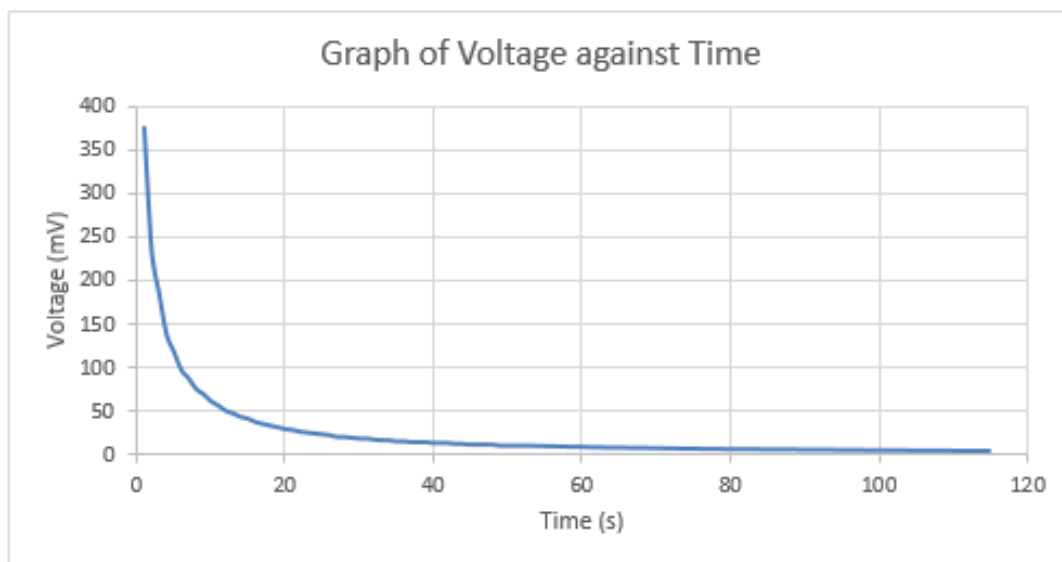


Figure 4.22: Discharge Curve of Capacitor

Figure 4.23 shows the discharge curve of the symmetric supercapacitor that was fabricated using synthesised  $FeCl_3 - GIC$ . The charging procedure for  $FeCl_3 - GIC$  supercapacitor was the same as the normal capacitor which was to charge for 10 minutes at 29 V. The discharge rate was plotted in a graph as shown in Figure 4.23.

From the discharge rate of  $FeCl_3 - GIC$  supercapacitor as shown in Figure 4.23. It can be observed that in the first 20 seconds, the supercapacitor discharged quickly from 472 mV to 192 mV. The supercapacitor was then discharged and stayed at around 150 mV.

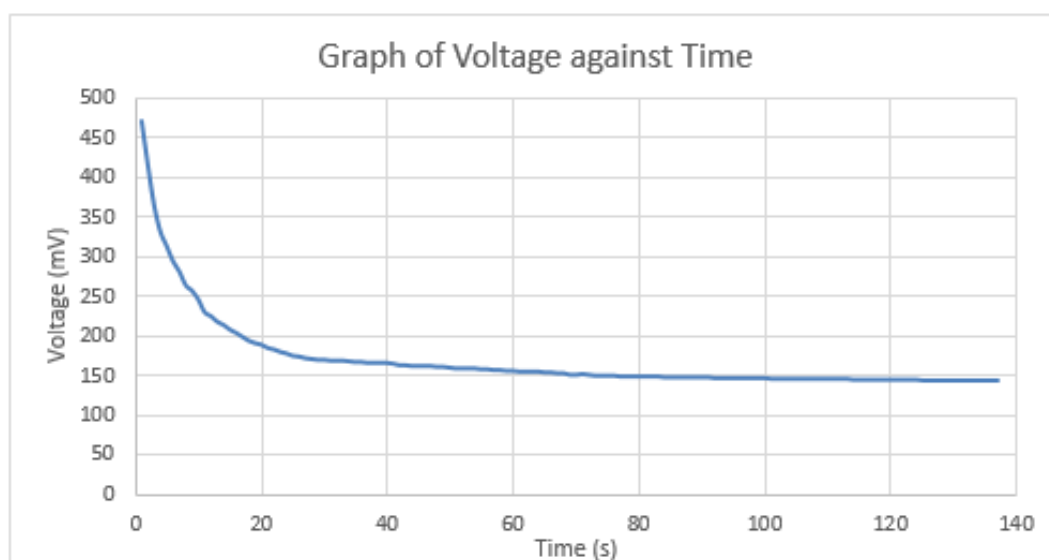


Figure 4.23: Discharge Curve of  $FeCl_3 - GIC$  Supercapacitor

Figure 4.24 shows the discharge rate of the symmetric supercapacitor that was constructed by using synthesised  $FeCl_3 - FLG$ . The charging process was the same as the previous capacitors, which were charged for 10 minutes at 29 V and the discharge rate was plotted in a graph as shown in Figure 4.24.

From Figure 4.24, it can be observed that the discharge curve of  $FeCl_3 - FLG$  supercapacitor was not as sharp as the discharge curve of the normal capacitor and  $FeCl_3 - GIC$  supercapacitor.  $FeCl_3 - FLG$  supercapacitor used 40 seconds to discharged from 818 mV to 433 mV. It was then discharged steadily and maintained at around 350 mV.

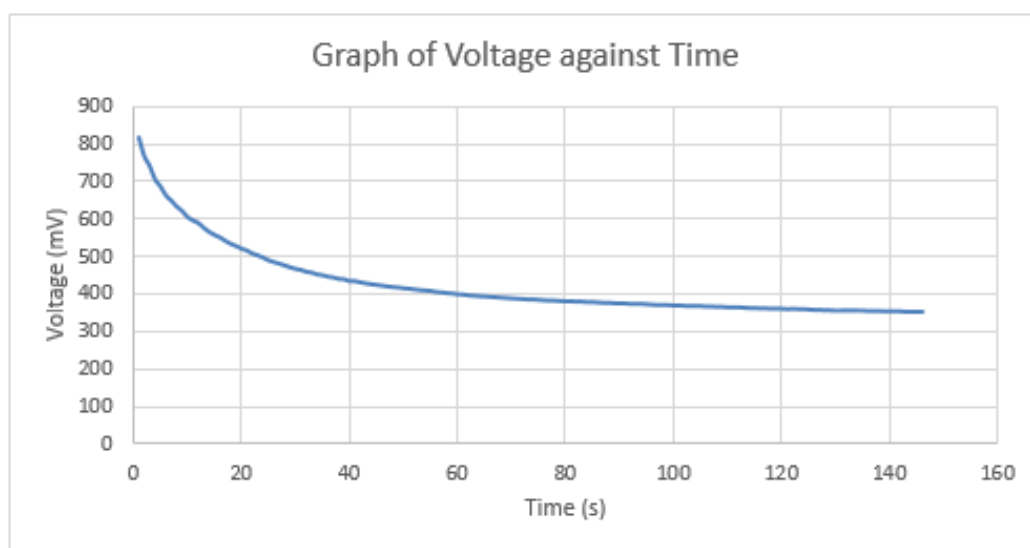


Figure 4.24: Discharge Curve of  $FeCl_3 - FLG$  Supercapacitor

Figure 4.25 shows the discharge curves of a normal capacitor,  $FeCl_3 - GIC$  and  $FeCl_3 - FLG$  supercapacitor. It can be observed that the total voltage can be stored in normal,  $FeCl_3 - GIC$  and  $FeCl_3 - FLG$  capacitor are 375 mV, 472 mV and 818 mV, respectively. A normal capacitor required 115 seconds to discharged and finally maintained at around 5 mV. Supercapacitor that was constructed by synthesised  $FeCl_3 - GIC$  needed 137 seconds to discharged and finally maintained at around 150 mV. Whereas,  $FeCl_3 - FLG$  supercapacitor required 146 seconds to discharged and maintained at around 350 mV.

From the discharge curves that was plotted in Figure 4.25, it can be summarised that the final discharged voltage of  $FeCl_3 - GIC$  supercapacitor was

about 30 times more than the normal capacitor, whereas  $FeCl_3 - FLG$  supercapacitor was about 70 times more than the normal capacitor. Therefore, the capacitor that was constructed using  $FeCl_3 - GIC$  and  $FeCl_3 - FLG$  can be known as supercapacitor due to the energy stored is more than 10 times of the normal capacitor. .

By comparing the maximum voltage stored, discharge rate and final discharged voltage, it can be concluded that the performance of  $FeCl_3 - FLG$  is better than  $FeCl_3 - GIC$ , and  $FeCl_3 - GIC$  is better than a normal capacitor.

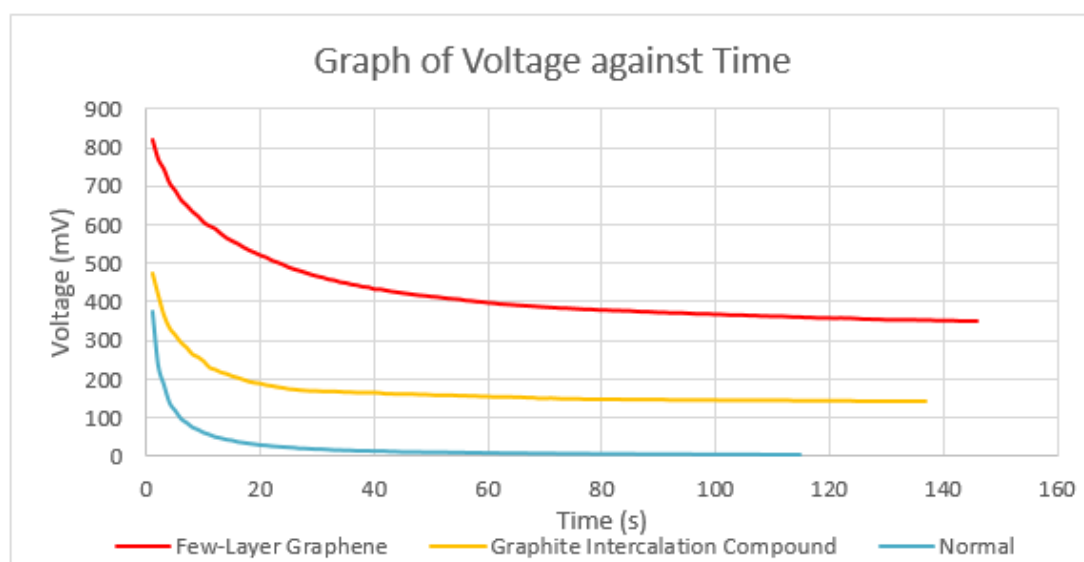


Figure 4.25: Discharge Curves of Normal Capacitor,  $FeCl_3 - GIC$  and  $FeCl_3 - FLG$  Supercapacitor

#### 4.4 Summary

From the SEM, FESEM, EDX, XRD and FTIR results, it can be concluded that  $FeCl_3 - GIC$  and  $FeCl_3 - FLG$  were successfully synthesised.  $FeCl_3 - GIC$  and  $FeCl_3 - FLG$  can be obtained through hydrothermal intercalation and microwave exfoliation method, however, hydrothermal intercalation method was more suitable for large quantity production. Whereas, microwave exfoliation method was suitable for laboratory research that require a small amount of sample in a short time. From the results of the performance of normal capacitor and supercapacitors, it can be summarised that the storage capacity of  $FeCl_3 - GIC$  supercapacitor was about 30 times more than the normal capacitor, whereas  $FeCl_3 - FLG$  supercapacitor was about 70 times more than the normal capacitor.

## CHAPTER 5

### CONCLUSION AND RECOMMENDATIONS

#### 5.1 Conclusion

The objectives of this project were achieved, iron (III) chloride ( $FeCl_3$ ) was successfully intercalated into the layered structure of graphite and exfoliate it mechanically and chemically through ultrasonication process.  $FeCl_3 - GIC$  was successfully synthesised by intercalating  $FeCl_3$  into the layered structure of graphite. The synthesised  $FeCl_3 - GIC$  was then undergone ultrasonication process to obtain  $FeCl_3 - FLG$ .

Furthermore,  $FeCl_3 - GIC$  and  $FeCl_3 - FLG$  were characterised by SEM, FESEM, EDX, XRD and FTIR. The results of SEM and FESEM show that there were  $FeCl_3$  intercalated between the layers of graphite and formed  $FeCl_3 - GIC$ . It also proved that the number of layer of  $FeCl_3 - FLG$  was between 2 to 5 layers.

Moreover, the results of SEM and FESEM can be supported by EDX and XRD. EDX and XRD results show that there were traces of carbon, iron oxide and chlorine found in both  $FeCl_3 - GIC$  and  $FeCl_3 - FLG$ . This prove that there are  $FeCl_3$  presented in both  $FeCl_3 - GIC$  and  $FeCl_3 - FLG$ . Besides, FTIR of  $FeCl_3 - GIC$  and  $FeCl_3 - FLG$  show that there were no functional group in both samples. Therefore, the possibility that the samples oxidised and formed GO was excluded.

In addition, the characteristic of supercapacitor that was constructed by synthesised  $FeCl_3 - GIC$  and  $FeCl_3 - FLG$  was determined. By comparing the performance of normal capacitor with the performance of supercapacitors that were constructed by synthesised  $FeCl_3 - GIC$  and  $FeCl_3 - FLG$ , the results show that  $FeCl_3 - GIC$  supercapacitor was able to stored 30 times more energy than normal capacitor and  $FeCl_3 - FLG$  supercapacitor was able to stored 70 times more energy than a normal capacitor.

In short, all the objectives of this project were accomplished, thus, the aim of this project which was to synthesis  $FeCl_3 - FLG$  by interlayer catalytic exfoliation for supercapacitor applications was successfully achieved as well.

## 5.2 Recommendations for Future Work

In this project, it had been proven that interlayer catalytic exfoliation was a method that was able to successfully synthesis  $FeCl_3 - GIC$  and  $FeCl_3 - FLG$ . However, the total amount that can be produced was low and it required a long production time. Therefore, it is strongly recommended to determine the method to synthesis  $FeCl_3 - FLG$  in large scale and reduce the time of production so that this technology can be produce in a large amount and adopt in current technology.

Next, the storage capacity of  $FeCl_3 - GIC$  and  $FeCl_3 - FLG$  had been proven to be very excellent. Thus, it is recommended to further improve the energy storage capacity of  $FeCl_3 - GIC$  and  $FeCl_3 - FLG$ .

Last but not least, it is also strongly recommended to explore other unique properties of  $FeCl_3 - GIC$  and  $FeCl_3 - FLG$ . As mentioned before in Chapter 1, it is also suitable to be apply in the field of biomedical, engineering, micromachine, electrical vehicle and electronics fields.

## REFERENCES

- Abouimrane, A., Compton, O.C., Amine, K. and Nguyen, S.T., 2010. Non-annealed graphene paper as a binder-free anode for lithium-ion batteries. *Journal of Physical Chemistry C*, 114(29), pp.12800–12804.
- Ali, G.A.M., Wahba, O.A.G., Hassan, A.M., Fouad, O.A. and Chong, K.F., 2015. Calcium-based nanosized mixed metal oxides for supercapacitor application. *Ceramics International*, [online] 41(6), pp.8230–8234.
- Alwarappan, S. and Pillai, 2011. *Graphene-Based Biosensors and Gas Sensors. Graphene: Synthesis and Applications*.
- Alymov, G., Vyurkov, V., Ryzhii, V. and Svintsov, D., 2016. Abrupt current switching in graphene bilayer tunnel transistors enabled by van Hove singularities. *Scientific Reports*, [online] 6(January), pp.1–8.
- Annett, J. and Cross, G.L.W., 2016. Self-assembly of graphene ribbons by spontaneous self-tearing and peeling from a substrate. *Nature*, [online] 535(7611), pp.271–275.
- Bernardo, A. and Di, 2017. P-wave triggered superconductivity in single-layer graphene on an electron-doped oxide superconductor. *Nature Communications*, [online] 8, pp.1–9.
- Chaudhuri, B., Bhadra, D., Moroni, L. and Pramanik, K., 2015. Myoblast differentiation of human mesenchymal stem cells on graphene oxide and electrospun graphene oxide-polymer composite fibrous meshes: Importance of graphene oxide conductivity and dielectric constant on their biocompatibility. *Biofabrication*, [online] 7(1), p.15009.
- Chu, K., Wang, X. hu, Li, Y. biao, Huang, D. jian, Geng, Z. rong, Zhao, X. long, Liu, H. and Zhang, H., 2018. Thermal properties of graphene/metal composites with aligned graphene. *Materials and Design*, [online] 140, pp.85–94.
- Chung-Ping Lai; Zhubei, 2017. *Method of making LED light bulb with graphene filament.pdf*.
- Ciesielski and Samorì, 2014. Grapheneviasonication assisted liquid-phase exfoliation. *Chem. Soc. Rev.*, [online] 43(1), pp.381–398.
- Dimiev, A.M., Ceriotti, G., Metzger, A., Kim, N.D. and Tour, J.M., 2016. Chemical mass production of graphene nanoplatelets in ~100% yield. *ACS Nano*, 10(1), pp.274–279.
- Diyar Sadyraliev, 2018. *Graphene Oxide - What Is It? - Nanografi Nano Technology*. [online] Nanografi Nano Technology. Available at: <<https://nanografi.com/blog/graphene-oxide-what-is-it/>> [Accessed 21 Aug. 2018].

Dong, L., Xu, C., Li, Y., Huang, Z.H., Kang, F., Yang, Q.H. and Zhao, X., 2016. Flexible electrodes and supercapacitors for wearable energy storage: A review by category. *Journal of Materials Chemistry A*, 4(13), pp.4659–4685.

El-Kady, M.F. and Kaner, R.B., 2013. Scalable fabrication of high-power graphene micro-supercapacitors for flexible and on-chip energy storage. *Nature Communications*, [online] 4, pp.1475–1479.

Emery, N., Hérold, C., Marêché, J.-F. and Lagrange, P., 2008. Synthesis and superconducting properties of CaC<sub>6</sub>. *Science and Technology of Advanced Materials*, [online] 9(4), p.044102.

Feng, L., Wang, K., Zhang, X., Sun, X., Li, C., Ge, X. and Ma, Y., 2017. Flexible Solid-State Supercapacitors with Enhanced Performance from Hierarchically Graphene Nanocomposite Electrodes and Ionic Liquid Incorporated Gel Polymer Electrolyte. *Advanced Functional Materials*, 28(4), pp.1–9.

Firouzabadi, H., Iranpoor, N., Jafari, A.A. and Jafari, M.R., 2008. Iron(III) trifluoroacetate [Fe(F<sub>3</sub>CCO<sub>2</sub>)<sub>3</sub>] as an easily available, non-hygroscopic, non-corrosive, highly stable and a reusable Lewis Acid catalyst: Efficient O-silylation of  $\alpha$ -hydroxyphosphonates, alcohols and phenols by hexamethyldisilazane (HMDS) under s. *Journal of Organometallic Chemistry*, 693(16), pp.2711–2714.

Frank, I.W., Tanenbaum, D.M., van der Zande, A.M. and McEuen, P.L., 2007. Mechanical properties of suspended graphene sheets. *Journal of Vacuum Science & Technology B: Microelectronics and Nanometer Structures Processing, Measurement, and Phenomena*, 25(6), pp.2558-2561.

Gaikwad, A.M., Whiting, G.L., Steingart, D.A. and Arias, A.C., 2011. Highly flexible, printed alkaline batteries based on mesh-embedded electrodes. *Advanced Materials*, 23(29), pp.3251–3255.

Galpaya, D., 2015. Synthesis, Characterization and Applications of Graphene Oxide-Polymer Nanocomposites. (June).

Geng, X., Guo, Y., Li, D., Li, W., Zhu, C., Wei, X., Chen, M., Gao, S., Qiu, S., Gong, Y., Wu, L., Long, M., Sun, M., Pan, G. and Liu, L., 2013. Interlayer catalytic exfoliation realizing scalable production of large-size pristine few-layer graphene. *Scientific Reports*, 3, pp.1–6.

Ghosh, S., Calizo, I., Teweldebrhan, D., Pokatilov, E.P., Nika, D.L., Balandin, A.A., Bao, W., Miao, F. and Lau, C.N., 2008. Extremely high thermal conductivity of graphene: Prospects for thermal management applications in nanoelectronic circuits. *Applied Physics Letters*, 92(15), pp.1–4.

Goh, M.S. and Pumera, M., 2010. Exhibiting Significant Advantages over Graphite Microparticles in Electroanalysis. *Analytical chemistry*, 82(19), pp.8367–8370.

Goldstein, J.I., Newbury, D.E., Michael, J.R., Ritchie, N.W.M., Scott, J.H.J. and Joy, D.C., 2017. Scanning electron microscopy and x-ray microanalysis. *Scanning Electron Microscopy and X-ray Microanalysis*, 34, pp.1–550.

Hernandez, Y., Nicolosi, V., Lotya, M., Blighe, F.M., Sun, Z., De, S., McGovern, I.T., Holland, B., Byrne, M., Gun'ko, Y.K., Boland, J.J., Niraj, P., Duesberg, G., Krishnamurthy, S., Goodhue, R., Hutchison, J., Scardaci, V., Ferrari, A.C. and Coleman, J.N., 2008. High-yield production of graphene by liquid-phase exfoliation of graphite. *Nature Nanotechnology*, 3(9), pp.563–568.

Hu, X., Li, Z. and Chen, J., 2017. Flexible Li-CO<sub>2</sub> Batteries with Liquid-Free Electrolyte. *Angewandte Chemie International Edition*, [online] 56(21), pp.5785–5789.

Kang, F., Zheng, Y.-P., Wang, H.-N., Nishi, Y. and Inagaki, M., 2002. Effect of preparation conditions on the characteristics of exfoliated graphite. *Carbon*, [online] 40(9), pp.1575–1581.

Kumar, R., Oh, J.H., Kim, H.J., Jung, J.H., Jung, C.H., Hong, W.G., Kim, H.J., Park, J.Y. and Oh, I.K., 2015. Nanohole-Structured and Palladium-Embedded 3D Porous Graphene for Ultrahigh Hydrogen Storage and CO Oxidation Multifunctionalities. *ACS Nano*, 9(7), pp.7343–7351.

Lalwani, G., D'Agati, M., Khan, A.M. and Sitharaman, B., 2016. Toxicology of graphene-based nanomaterials. *Advanced Drug Delivery Reviews*, [online] 105(February 2018), pp.109–144.

Liu, Y., Liang, H., Xu, Z., Xi, J., Chen, G., Gao, W., Xue, M. and Gao, C., 2017. Superconducting Continuous Graphene Fibers via Calcium Intercalation. *ACS Nano*, 11(4), pp.4301–4306.

López, María del Prado Lavín; Palomino, José Luis Valverde; Silva, María Luz Sánchez; Izquierdo, A.R., 2018. Optimization of the Synthesis Procedures of Graphene and Graphene Oxide. *Intech open*, 2, p.64.

Nardecchia, S., Carriazo, D., Ferrer, M.L., Gutiérrez, M.C. and Del Monte, F., 2012. Three dimensional macroporous architectures and aerogels built of carbon nanotubes and/or graphene: Synthesis and applications. *Chemical Society Reviews*, 42(2), pp.794–830.

Nicolosi, V., Chhowalla, M., Kanatzidis, M.G., Strano, M.S. and Coleman, J.N., 2013. Liquid exfoliation of layered materials. *Science*, 340(6139), pp.72–75.

Novoselov, K.S., Geim, A.K., Morozov, S. V, Jiang, D., Zhang, Y., Dubonos, S. V, Grigorieva, I. V and Firsov, A.A., 2004. Electric Field Effect in Atomically Thin Carbon Films. *Source: Science, New Series Gene Expression: Genes in Action*, [online] 306(5696), pp.666–669.

Oh, J.Y., Rondeau-Gagné, S., Chiu, Y.C., Chortos, A., Lissel, F., Wang, G.J.N., Schroeder, B.C., Kurosawa, T., Lopez, J., Katsumata, T., Xu, J., Zhu, C., Gu, X., Bae, W.G., Kim, Y., Jin, L., Chung, J.W., Tok, J.B.H. and Bao, Z., 2016. Intrinsically

stretchable and healable semiconducting polymer for organic transistors. *Nature*, [online] 539(7629), pp.411–415.

Ozturk, Z., Baykasoglu, C. and Kirca, M., 2016. Sandwiched graphene-fullerene composite: A novel 3-D nanostructured material for hydrogen storage. *International Journal of Hydrogen Energy*, [online] 41(15), pp.6403–6411.

Papageorgiou, D.G., Kinloch, I.A. and Young, R.J., 2017. Mechanical properties of graphene and graphene-based nanocomposites. *Progress in Materials Science*, [online] 90, pp.75–127.

Paton, K.R., Varrla, E., Backes, C., Smith, R.J., Khan, U., O'Neill, A., Boland, C., Lotya, M., Istrate, O.M., King, P., Higgins, T., Barwich, S., May, P., Puczkarski, P., Ahmed, I., Moebius, M., Pettersson, H., Long, E., Coelho, J., O'Brien, S.E., McGuire, E.K., Sanchez, B.M., Duesberg, G.S., McEvoy, N., Pennycook, T.J., Downing, C., Crossley, A., Nicolosi, V. and Coleman, J.N., 2014. Scalable production of large quantities of defect-free few-layer graphene by shear exfoliation in liquids. *Nature Materials*, 13(6), pp.624–630.

Qi, X., Qu, J., Zhang, H. Bin, Yang, D., Yu, Y., Chi, C. and Yu, Z.Z., 2015. FeCl<sub>3</sub> intercalated few-layer graphene for high lithium-ion storage performance. *Journal of Materials Chemistry A*, 3(30), pp.15498–15504.

Qie, L., Lin, Y., Connell, J.W., Xu, J. and Dai, L., 2017. Highly Rechargeable Lithium-CO<sub>2</sub>Batteries with a Boron- and Nitrogen-Codoped Holey-Graphene Cathode. *Angewandte Chemie - International Edition*, 56(24), pp.6970–6974.

Raji, A.R.O., Villegas Salvatierra, R., Kim, N.D., Fan, X., Li, Y., Silva, G.A.L., Sha, J. and Tour, J.M., 2017. Lithium Batteries with Nearly Maximum Metal Storage. *ACS Nano*, 11(6), pp.6362–6369.

Rattana, T., Chaiyakun, S., Witit-Anun, N., Nuntawong, N., Chindaudom, P., Oaew, S., Kedkeaw, C. and Limsuwan, P., 2012. Preparation and characterization of graphene oxide nanosheets. *Procedia Engineering*, [online] 32, pp.759–764.

Ren, S., Rong, P. and Yu, Q., 2018. Preparations, properties and applications of graphene in functional devices: A concise review. *Ceramics International*, 44(11), pp.11940–11955.

Salvatore, M., 2017. Synthesis and Characterization of Expandable Graphite using different Oxidizing Agents.

Shayeganfar, F. and Shahsavari, R., 2016. Oxygen- and Lithium-Doped Hybrid Boron-Nitride/Carbon Networks for Hydrogen Storage. *Langmuir*, 32(50), pp.13313–13321.

Shornikova, O.N., Dunaev, A. V., Maksimova, N. V. and Avdeev, V. V., 2006. Synthesis and properties of ternary GIC with iron or copper chlorides. *Journal of Physics and Chemistry of Solids*, 67(5–6), pp.1193–1197.

Son, I.H., Park, J.H., Park, S., Park, K., Han, S., Shin, J., Doo, S.G., Hwang, Y., Chang, H. and Choi, J.W., 2017. Graphene balls for lithium rechargeable batteries with fast charging and high volumetric energy densities. *Nature Communications*, [online] 8(1), pp.1–10.

Tao, L.Q., Tian, H., Liu, Y., Ju, Z.Y., Pang, Y., Chen, Y.Q., Wang, D.Y., Tian, X.G., Yan, J.C., Deng, N.Q., Yang, Y. and Ren, T.L., 2017. An intelligent artificial throat with sound-sensing ability based on laser induced graphene. *Nature Communications*, [online] 8, pp.1–8.

Teng, C., Xie, D., Wang, J., Yang, Z., Ren, G. and Zhu, Y., 2017. Ultrahigh Conductive Graphene Paper Based on Ball-Milling Exfoliated Graphene. *Advanced Functional Materials*, 27(20).

Tian, H., Li, C., Mohammad, M.A., Cui, Y.L., Mi, W.T., Yang, Y., Xie, D. and Ren, T.L., 2014. Graphene earphones: Entertainment for both humans and animals. *ACS Nano*, 8(6), pp.5883–5890.

Tiwari, S.K., Kumar, V., Huczko, A., Oraon, R., Adhikari, A. De and Nayak, G.C., 2016. Magical Allotropes of Carbon: Prospects and Applications. *Critical Reviews in Solid State and Materials Sciences*, 41(4), pp.257–317.

Van Heerden, X. and Badenhorst, H., 2015. The influence of three different intercalation techniques on the microstructure of exfoliated graphite. *Carbon*, [online] 88, pp.173–184.

Wang, L., Zhu, Y., Guo, C., Zhu, X., Liang, J. and Qian, Y., 2014. Ferric chloride-graphite intercalation compounds as anode materials for Li-ion batteries. *ChemSusChem*, 7(1), pp.87–91.

Wang, S., Wang, C. and Ji, X., 2017. Towards understanding the salt-intercalation exfoliation of graphite into graphene. *RSC Advances*, 7(82), pp.52252–52260.

Wei, T., Fan, Z., Luo, G., Zheng, C. and Xie, D., 2009. A rapid and efficient method to prepare exfoliated graphite by microwave irradiation. *Carbon*, 47(1), pp.337–339.

Wen, L., Li, F. and Cheng, H.-M., 2016. Carbon Nanotubes and Graphene for Flexible Electrochemical Energy Storage: from Materials to Devices. *Advanced Materials*, [online] 28(22), pp.4306–4337.

Whitener, K.E. and Sheehan, P.E., 2014. Graphene synthesis. *Diamond and Related Materials*, [online] 46, pp.25–34.

Xiao, H., Wu, Z.S., Chen, L., Zhou, F., Zheng, S., Ren, W., Cheng, H.M. and Bao, X., 2017. One-Step Device Fabrication of Phosphorene and Graphene Interdigital Micro-Supercapacitors with High Energy Density. *ACS Nano*, 11(7), pp.7284–7292.

Xu, J., Hu, J., Li, Q., Wang, R., Li, W., Guo, Y., Zhu, Y., Liu, F., Ullah, Z., Dong, G., Zeng, Z. and Liu, L., 2017. Fast Batch Production of High-Quality Graphene Films in a Sealed Thermal Molecular Movement System. *Small*, 13(27), pp.8–11.

Xu, J., Dou, Y., Wei, Z., Ma, J., Deng, Y., Li, Y., Liu, H. and Dou, S., 2017. Recent Progress in Graphite Intercalation Compounds for Rechargeable Metal (Li, Na, K, Al)-Ion Batteries. *Advanced Science*, 4(10).

Xu, X., Zhang, Z., Qiu, L., Zhuang, J., Zhang, L., Wang, H., Liao, C., Song, H., Qiao, R., Gao, P., Hu, Z., Liao, L., Liao, Z., Yu, D., Wang, E., Ding, F., Peng, H. and Liu, K., 2016. Ultrafast growth of single-crystal graphene assisted by a continuous oxygen supply. *Nature Nanotechnology*, [online] 11(11), pp.930–935.

Yang, X., Wang, Y., Huang, X., Ma, Y., Huang, Y., Yang, R., Duan, H. and Chen, Y., 2011. Multi-functionalized graphene oxide based anticancer drug-carrier with dual-targeting function and pH-sensitivity. *Journal of Materials Chemistry*, 21(10), pp.3448–3454.

Yoon, G., Seo, D.H., Ku, K., Kim, J., Jeon, S. and Kang, K., 2015. Factors affecting the exfoliation of graphite intercalation compounds for graphene synthesis. *Chemistry of Materials*, 27(6), pp.2067–2073.

Zheng, G., Chen, Y., Huang, H., Zhao, C., Lu, S., Chen, S., Zhang, H. and Wen, S., 2013. Improved transfer quality of CVD-grown graphene by ultrasonic processing of target substrates: Applications for ultra-fast laser photonics. *ACS Applied Materials and Interfaces*, 5(20), pp.10288–10293.

Zhou, C., Szpunar, J.A. and Cui, X., 2016. Synthesis of Ni/Graphene Nanocomposite for Hydrogen Storage. *ACS Applied Materials and Interfaces*, 8(24), pp.15232–15241.

Zhu Jiping , Chen Zuyao, W.C., 2003. Preparation and characterization of CuCl<sub>2</sub>–FeCl<sub>3</sub>–H<sub>2</sub>SO<sub>4</sub>–graphite intercalation compounds by hydrothermal synthesis. *elsevier*, 52(2), pp.507–513.

## APPENDICES

### APPENDIX A: Results of Normal Capacitor, FeCl<sub>3</sub>-GIC Supercapacitor and FeCl<sub>3</sub>-FLG Supercapacitor

Time (s)	Voltage (mV)		
	Normal Capacitor	FeCl <sub>3</sub> -GIC Supercapacitor	FeCl <sub>3</sub> -FLG Supercapacitor
1	375	472	818
2	234	416	768
3	185	365	742
4	138	332	706
5	118	314	687
6	97	295	663
7	87	282	649
8	75	265	633
9	69	258	621
10	61	247	605
11	56	231	596
12	50	226	589
13	47	219	576
14	43	215	565
15	41	209	557
16	37	205	550
17	35	200	541
18	33	195	533
19	31	192	527
20	29	190	520
21	28	186	515
22	26	184	507
23	25	181	502
24	24	179	496
25	23	176	489
26	22	175	484
27	20	173	480
28	20	172	475
29	19	171	470
30	18	171	466
31	18	170	463
32	17	170	458
33	16	170	456
34	16	169	451
35	15	168	449
36	15	168	445

37	14	167	443
38	14	167	439
39	14	167	438
40	13	167	433
41	13	166	433
42	13	164	430
43	12	164	427
44	12	163	425
45	11	163	423
46	11	163	421
47	11	163	419
48	11	162	417
49	10	162	416
50	10	161	414
51	10	160	413
52	10	160	411
53	10	160	409
54	9.6	160	408
55	9.5	159	407
56	9.3	159	404
57	9.1	158	403
58	8.9	158	401
59	8.7	157	400
60	8.5	157	398
61	8.3	156	397
62	8.1	156	395
63	7.9	156	394
64	7.8	156	393
65	7.8	155	392
66	7.7	155	391
67	7.5	154	390
68	7.3	154	389
69	7.3	152	388
70	7.2	152	387
71	7	153	386
72	6.8	152	385
73	6.7	151	384
74	6.6	151	384
75	6.5	151	383
76	6.4	151	382
77	6.3	150	381
78	6.2	150	381
79	6.1	150	380
80	6	150	379
81	6	150	379
82	5.8	150	378

83	5.8	150	378
84	5.7	149	377
85	5.6	149	377
86	5.6	149	376
87	5.5	149	375
88	5.4	149	375
89	5.4	149	374
90	5.3	149	373
91	5.2	149	373
92	5.2	148	372
93	5.1	148	372
94	5.1	148	372
95	5	148	371
96	5	148	370
97	4.9	148	369
98	4.8	148	369
99	4.7	148	369
100	4.7	148	368
101	4.7	147	368
102	4.6	147	367
103	4.5	147	366
104	4.5	147	366
105	4.4	147	366
106	4.3	147	365
107	4.3	147	365
108	4.3	147	364
109	4.2	147	364
110	4.2	147	363
111	4.1	147	363
112	4	147	363
113	4	147	362
114	4	146	361
115	4	146	361
116	-	146	360
117	-	146	360
118	-	146	359
119	-	146	359
120	-	146	359
121	-	146	358
122	-	146	359
123	-	146	358
124	-	146	358
125	-	145	357
126	-	145	356
127	-	145	356
128	-	145	355

129	-	145	355
130	-	145	354
131	-	145	354
132	-	145	354
133	-	145	354
134	-	145	354
135	-	145	354
136	-	145	353
137	-	145	353
138	-	-	353
139	-	-	352
140	-	-	352
141	-	-	352
142	-	-	352
143	-	-	351
144	-	-	351
145	-	-	351
146	-	-	351

---